transcriptional factors [3]. Successful suppression of transcription by Py-Im polyamides has been demonstrated for several genes [4]. In the current study, we synthesized three Py-Im hairpin polyamides against sequences flanking the HRE of the human VEGF gene. A combination of three Py-Im hairpin polyamides suppressed HIF-induced transcription in reporter assays and successfully suppressed transcription and translation of the VEGF gene in A498 cells.

Materials and methods

Determination of target sequences

On the basis of the rules of sequence-recognition by Py-Im polyamides [4–6], we designed three Py-Im hairpin polyamides targeting 4–5-base-pair sequences flanking the HRE of the human VEGF gene (Figure 1). Target sequences were set between A/T or T/A pairs according to the reported sequences that successfully suppressed other transcriptional factors [4]. For A/T or T/A, we used a β-alanine pair that degenerately recognizes these base pairs and increases the affinity of the polyamides to the target sequences by correcting intramolecular distortion [7].

Preparation of pyrrole-imidazole hairpin polyamides

N-methylpyrrole (Py)-*N*-methylimidazole (Im) polyamides were synthesized by using a previously described Fmoc solid-phase method [8]. Polyamides were purified by high performance liquid chromatography (HPLC) with a Jasco PU-980 HPLC pump, a UV-975 HPLC UV/VIS detector, and a Chemcobond 5-ODS-H column (4.6 mm × 150 mm). HPLC was performed using 0.1% acetic acid and a linear gradient (20–30% for polyamide no. 1, 10–50% for polyamide no. 2, and 20–30% for polyamide no. 3) of acetonitrile at a flow rate of 1.0 ml/min with detection at 254 nm. Polyamides were eluted at 30.0 min. Structures of the synthesized polyamides were verified by electron spray ionization mass spectra (ESIMS) recorded on a PE Sciex API 165 mass spectrometer. Molecular weights of polyamides measured by ESIMS are listed in Table I. Synthesized polyamides were lyophilized and stored at −20°C, and dissolved in dimethylsulfoxide for the experiments.

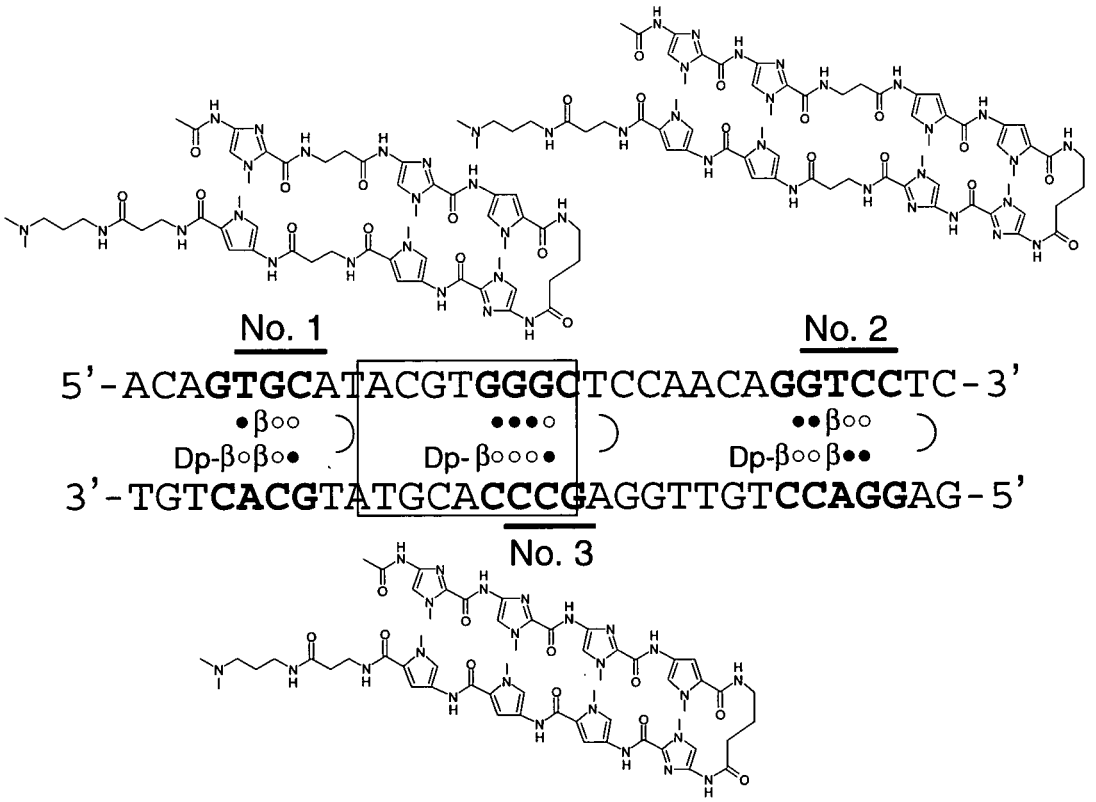

Figure 1. Target sequences and chemical structures of the *N*-methylpyrrole-*N*-methylimidazole hairpin polyamides. Consensus binding site for HIF is indicated by an open box. Open and closed circles represent imidazole and pyrrole rings, respectively. Dp and b denote dimethylaminopropylamine and b-alanine residues, respectively.

Table I. Molecular weights of polyamides measured by ESIMS.

Polyamide	Composition formula	Molecular weight	
		Calculated	Observed
No. 1	$C_{53}H_{71}N_{21}O_{11}$ $[M^+ + H]$	1177.56	1178.27
No. 2	$C_{64}H_{82}N_{26}O_{13}$ $[M^+ + H]$	1422.66	1423.50
No. 3	$C_{58}H_{72}N_{24}O_{11}$ $[M^+ + H]$	1280.58	1281.35

ESIMS, electron spray ionization mass spectra.

Cells and culture conditions

A498 is an established cell line of undifferentiated renal cell carcinoma (American Type Culture Collection, Manassas, VA, USA) that lacks normal expression of the von Hippel-Lindau gene because of a frame-shift mutation at codon 213 [9]. High-level expressions of HIF-1α and HIF-2α in A498 have been demonstrated [10]. 293 is an immortalized human fetal kidney epithelial cell line with very low levels of HIF-1α and HIF-2α under normoxic conditions [10]. Cells were cultured in Dulbecco's modified Eagle's medium (DMEM; Sigma Aldrich, St. Louis, MO, USA) containing 10% fetal bovine serum in a humid chamber with 5% CO_2 at 37°C.

Plasmids

The following plasmids were used to evaluate the effects of the hairpin polyamides on HIF-1α-induced transcription: p(HA)HIF-1α (401Δ603), HA-tagged full-length human HIF-1α with internal deletion of oxygen-dependent degradation domain [11–13]; pTRE-EPAS, full-length human HIF-2α [10]; pARNT, full-length human ARNT [11–13]; pGL3VEGF, pGL3 promoter (Promega, Madison, WI, USA) containing the 385-bp VEGF promoter sequence (−1175 to −790) [14]; pCMVβ (BD biosciences, Palo Alto, CA, USA), a full-length human β-galactosidase cDNA.

Reporter assay

Two hundred and ninety three cells were seeded in 12-well plates (15×10^4 cells per well) and cultured in a humid chamber (5% CO_2). Twenty-four hours later, 0.25 μg of pGL3VEGF, 0.1 μg of p(HA)HIF1α(401Δ 603) or pTRE-EPAS, and 0.1 μg of pARNT were transiently transfected using the FuGene transfection reagent (Roche Applied Science, Penzberg, Germany) according to the manufacturer's protocol. pCMVβ (0.1 μg) was also transfected as a reference plasmid. Two hours later, synthesized polyamides were added to the culture. Doses and combinations of the polyamides are shown in the figures. After incubation for another 24 h, cells were lyzed with M-PER reagent (Pierce, Rockford, IL, USA). Luciferase activity was determined with the Bright-Glo™ Luciferase assay system (Promega, Madison, WI, USA). The luminescence signal was evaluated by using a Gene Light 55 luminometer (Microtec, Tokyo, Japan). The activity of β-galactosidase was measured by using a mammalian β-galactosidase assay kit (Pierce, Rockford, IL, USA) and an MT Max microplate reader (Wako, Tokyo, Japan). Assays were carried out in triplicate and repeated at least twice. The results were expressed as a ratio of luciferase activity to β-galactosidase activity.

Real-time reverse transcriptase-polymerase chain reaction

A498 cells were seeded in 6-well plates (30×10^4/well). The medium was replaced 24 h later and a polyamide mixture (5 μM in total) was added to the culture. Total RNA was extracted from the cells after 24, 48, and 72 h using ISOGEN (Nippon Gene, Tokyo, Japan), an RNA-isolating reagent. cDNA was synthesized from 5 μg of the total RNA samples using the SuperScript™ First-Strand Synthesis System for reverse transcriptase-polymerase chain reaction (RT-PCR; Invitrogen, Carlsbad, CA, USA). Five microliters of 500-fold-diluted cDNA samples were subjected to real time PCR by using a Light Cycler™ real time PCR instrument (Roche Applied Science, Penzberg, Germany). Light Cycler™ primer sets for human VEGF or human GAPDH (Serach LC, Heidelberg, Germany) were used together with LightCycler FastStart DNA Master SYBR Green I (Roche Applied Science, Penzberg, Germany). Results were expressed as a ratio of VEGF mRNA to GAPDH mRNA. Experiments were carried out in triplicate and repeated at least twice.

Enzyme-linked immunosorbent assay

A498 cells were plated on 24-well plates (5×10^4/well). The medium was replaced 24 h later and a polyamide mixture (5 μM in total) was added to the culture. Conditioned media were collected after 24, 48 and 72 h. The concentration of VEGF in the conditioned media was measured by using a Cytokine Enzyme-Linked Immunosorbent Assay (ELISA) Human VEGF Kit (American Research Products, Belmont, MA, USA). Assays were carried out in triplicate and repeated at least twice. Results were expressed as a ratio of VEGF concentration to total protein concentration, which was determined by using the BCA™ Protein Assay Kit (Pierce, Rockford, IL, USA).

Cell viability assay

A498 or 293 cells were seeded in 24-well plates. The medium was replaced 24 h later and polyamides at designated concentrations were added to the culture. After 24 h of incubation, the viability of the cells was assessed by using a CellTiter 96 AQueous One Solution Cell Proliferation Assay reagent (Promega, Madison, WI, USA). For A498, viability at 48 and 72 h was also measured. All assays were carried out in triplicate and repeated at least twice.

Electrophoresis mobility shift assay

Nuclear extract (100 μl) was prepared from 1×10^6 A498 cells using the NE-PER Nuclear and Cytoplasmic Extraction Reagent (Pierce, Rockford, IL, USA) according to the manufacturer's instructions. The binding reaction was carried out by using a Light-Shift Chemiluminescent Electrophoresis Mobility Shift Assay (EMSA) Kit (Pierce, Rockford, IL, USA). Twenty femtomoles of a biotin-labeled double-stranded oligonucleotide (5′-GTGCATACGTGGGCTCCAACAGGTCC-3′) corresponding to the sequence harboring the HRE of the human VEGF gene was mixed with 10 nmol of the polyamide mixture (no. 1, 2 or 3) or a polyamide targeting the human telomere sequence (TTAGGG) [15] in 20 μl of 1x binding buffer containing 2.5% glycerol, 5 mM $MgCl_2$, 50 ng/μl poly(dIdC), and 0.05% NP40. The reaction mixture was incubated for 20 min at room temperature, mixed with 2 μl of the A498 nuclear extract, and then incubated for another 20 min at room temperature. The nuclear extract was substituted with an equal volume of H_2O in a negative control. In a positive control, polyamide samples were replaced by an equal volume of H_2O. The reaction products were mixed with 5x loading buffer, electrophoresed in a 6% polyacrylamide gel (Invitrogen, Carlsbad, CA, USA) in 0.5x Tris-borate-EDTA (TBE), and transferred to a nylon membrane (Pierce, Rockford, IL, USA). Biotin-labeled DNA was detected by using a Chemiluminescent Nucleic Acid Detection Module (Pierce, Rockford, IL, USA) according to the manufacturer's instructions and analyzed by using an LAS-1000 imaging system (Fujifilm, Tokyo, Japan).

Results

Dose-dependent suppression of HIF-1α-induced transcription by polyamide mixture

We evaluated the effects of the synthesized polyamides on HIF-1α -induced transcription by using a reporter assay. A luciferase-expressing vector with the promoter region of the human VEGF gene was used as a reporter plasmid. Because HIF-1α is fairly unstable under normal oxygen tension, we used a stable HIF-1α construct that is transcriptionally active. Because HIF-1α makes a heterodimer with ARNT (also known as HIF-1α) for binding to the HRE, a plasmid clone of the human ARNT gene was transfected along with the HIF-1α. A plasmid containing the human β-galactosidase gene was also transfected and used as a reference standard. As shown in Figure 2, a combination of three hairpin polyamides suppressed transcription induced by HIF-1α in a dose-dependent manner to 56% of the control (vehicle only). The viability of the cells was not affected.

Suppression of HIF-1α-induced transcription by a combination of the three hairpin polyamides

The effects of each polyamide alone and various combinations of the three polyamides were evaluated by using a reporter assay. As shown in Figure 3, of the three polyamides, no.2 was the most potent suppressor of HIF-induced transcription at a concentration of 5 μM. A combination of all three polyamides, however, resulted in satisfactory

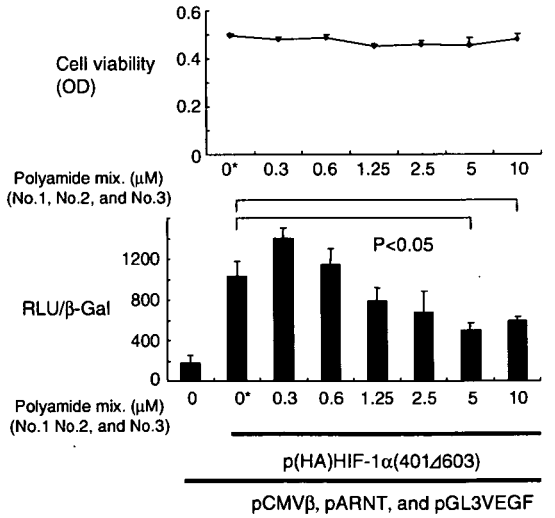

Figure 2. Dose-dependent inhibition of HIF-1α-induced transcription in 293 cells. Cells were transfected with plasmids coding hypoxia-stable HIF-1α, ARNT, and β-galactosidase, along with a reporter plasmid (pGL3VEGF), and then treated with the mixture of three pyrrole-imidazole hairpin polyamides for 24 h. Transcriptional activity was measured and expressed as a ratio of luciferase to β-galactosidase activity. Statistically significant suppression of transcription was noted at a concentration of 5 μM or greater. Cell viability was not affected by the polyamides. RLU and β-Gal denote relative luciferase units and β-galactosidase activity, respectively. OD: optical density. *: Vehicle (dimethylsulfoxide) only.

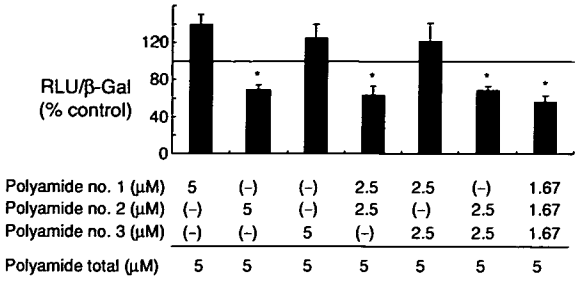

Figure 3. Effects of combinations of the three polyamides on HIF-1α -induced transcription in 293 cells. Cells were transfected with plasmids coding for hypoxia-stable HIF-1α(p(HA) HIF-1α(401Δ603)), ARNT (pARNT), and β-galactosidase (pCMVβ), along with a reporter plasmid (pGL3VEGF), and then incubated with a particular combination of the pyrrole-imidazole polyamides for 24 h. Transcriptional activity was expressed as a ratio of luciferase to β-galactosidase activity. A statistically significant reduction in transcription was achieved by applying all three Py-Im hairpin polyamides. A similar suppression was observed when polyamide no. 3 was applied alone or together with either polyamide no. 1 or no. 2. Cell viability was not affected by the treatment. RLU and β-Gal represent relative luciferase units and β-galactosidase activity, respectively. *:P <0.05 compared with controls.

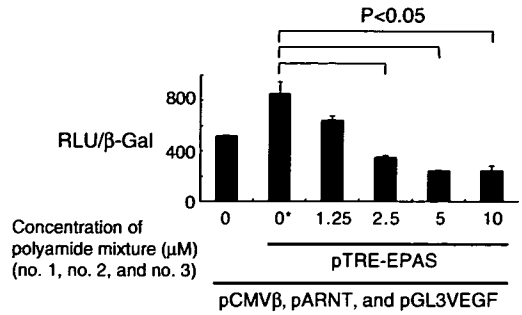

Figure 4. Dose-dependent inhibition of HIF-2α-induced transcription in 293 cells. Cells were transfected with plasmids coding full-length HIF-2α (pTRE-EPAS), ARNT(pARNT), and β-galactosidase (pCMVβ), along with a reporter plasmid (pGL3VEGF), and then treated with a mixture of the three pyrrole-imidazole hairpin polyamides for 24 h. Transcriptional activity was measured and expressed as a ratio of luciferase to β-galactosidase activity. Statistically significant suppression of transcription was noted at a concentration of 2.5 μM or greater. RLU and β-Gal denote relative luciferase units and β-galactosidase activity, respectively. *: Vehicle (dimethylsulfoxide) only.

suppression at lower concentrations of each polyamide compared with the monotreatment.

Suppression of HIF-2α-induced transcription by the polyamide mixture

We also examined the effects of the polyamide mixture on HIF-2α-induced transcription by using a reporter assay. A luciferase-expressing vector with the promoter region of the human VEGF gene was used as a reporter plasmid. As in the experiments using HIF-1α, a plasmid clone of the human ARNT gene was co-transfected with a full-length clone of the human HIF-2α gene. A plasmid containing the human β-galactosidase gene was also transfected and used as a reference standard. As shown in Figure 4, a combination of the three hairpin polyamides suppressed transcription induced by HIF-2α in a dose-dependent manner to 28% of the control (vehicle only).

Suppression of transcription and secretion of VEGF in renal cell carcinoma cells by the polyamide mixture

We examined the effects of the mixture of all three polyamides on VEGF transcription in renal cell carcinoma cells by using real-time RT-PCR. GAPDH mRNA was used as an internal standard. We used A498, a cell line derived from human renal cell carcinoma, with a frame-shift mutation in the VEGF gene. As shown in Figure 5, the polyamide mixture at a concentration of 5 μM inhibited VEGF transcription in A498 cells in a time-dependent manner. An approximately 50% reduction in VEGF transcription relative to the control (vehicle only) was observed when cells were exposed to the polyamide mixture for 72 h. Inhibition of VEGF at the protein level was examined by ELISA using conditioned media. The results were consistent with those of real-time RT-PCR. Secretion of VEGF was suppressed by the polyamide mixture in a time-dependent manner. The amount of VEGF in the conditioned media was reduced to approximately 50% of the control (vehicle only) by exposing A498 cells to the polyamide mixture for 72 h. The viability of A498 cells was not affected by incubation with the Py-Im polyamides.

Specific inhibition of HIF-HRE binding by the polyamide mixture

EMSA was carried out to confirm the inhibitory effects of the polyamide mixture on HIF-HRE binding (Figure 6). Addition of the A498 nuclear extract to the reaction mixture caused an apparent mobility shift of the biotin-labeled DNA, which was suppressed by the polyamide mixture recognizing the human HRE. The mobility shift was not affected by a polyamide recognizing the human telomere sequence, which was used as a control.

Statistics

Each assay was carried out in triplicate and repeated at least twice. Statistical significance was analyzed by using Student's t-test.

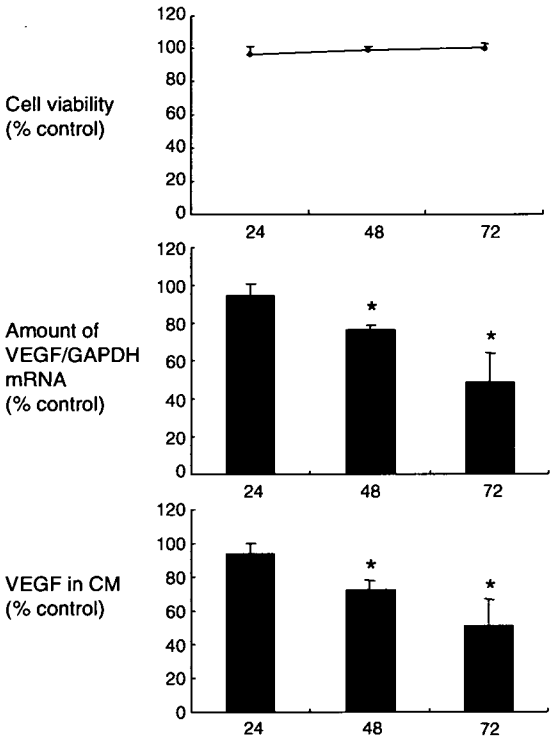

Figure 5. Suppressive effects of the mixture of three Py-Im hairpin polyamides on VEGF transcription and secretion in A498, a renal cell carcinoma cell line. Cells were treated with the mixture of three pyrrole-imidazole polyamides (5 mM in total) for 24–72 h. Transcription of the VEGF gene was evaluated by real time RT-PCR. The results were expressed as a ratio of VEGF mRNA to GAPDH mRNA. An approximately 50% reduction in transcription was observed after 72 h treatment. Consistently, VEGF secreted in conditioned medium (CM) decreased by approximately 50% compared with the control. *: $P<0.05$ compared with controls.

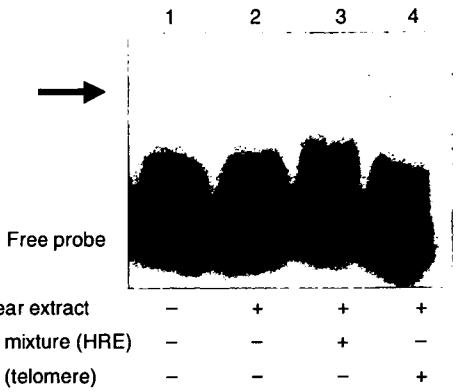

Figure 6. Inhibitory effects of pyrrole-imidazole hairpin polyamides on the HIF-HRE interaction were evaluated by using an electrophoresis mobility shift assay. Nuclear extract of A498 human renal cell cancer cells caused a mobility shift (arrow) of a biotin-labeled double-stranded oligonucleotide corresponding to human HRE (lanes 1 and 2). The polyamide mixture against the HRE suppressed the mobility shift (lane 3), which was not affected by a polyamide recognizing the human telomere sequence (lane 4).

Discussion

VEGF transcription in renal cell carcinoma cells was effectively suppressed by the Py-Im hairpin polyamides in the current study. Inhibition of the HIF-HRE interaction was confirmed by EMSA to be the underlying mechanism of this suppression. The hairpin polyamide strategy was pioneered by Dervan and colleagues [3]. Py and Im covalently link side-by-side in an anti-parallel arrangement that has been shown to recognize and bind to specific DNA sequences [4–6]. Im-Py recognizes G:C, whereas Py-Im recognizes C:G. The Py-Py pair recognizes A:T or T:A base pairs. The hydroxypyrrole and Py pair (Hp–Py) distinguishes T:A from A:T and vice versa. Placing a β-alanine pair, which degenerately binds to T:A or A:T, increases the affinity and specificity for sequences by relaxing the rigid curvature of polyamides [7]. Following these rules, regulation of gene expression by Py-Im hairpin polyamides has been successfully demonstrated for a variety of transcriptional factors, including Ets-1, TATA box (TBP) binding protein and lymphoid enhancer factor (LEF) 1 [4]. Our data suggest that HIF-induced transcription can also be controlled effectively by competitive binding of multiple Py-Im hairpin polyamides.

In the current study, we prepared three polyamides recognizing 4–5 base pairs flanking the HRE of the VEGF gene, and administered them together to obtain maximum specificity. Because of technical constraints, it is difficult to synthesize long polyamide chains. Moreover, the longer the target sequence is, the greater the intramolecular distortion becomes. Thus, Py-Im hairpin polyamides against 4–5-base-pair sequences have been used in most studies. Recently, a hairpin polyamide that recognizes TACG within the HRE has been reported to inhibit VEGF transcription [16]. Treatment with a combination of multiple polyamides is another option, and may increase the efficacy of treatment with Py-Im hairpin polyamides.

Py-Im hairpin polyamides have advantages as modulators of gene expression [4]. First, their low molecular weight allows them to permeate through cell membranes: they simply pass through cell membranes and reach their target sites without special aids or vehicles such as expression vectors or liposomes. Designing hairpin polyamides is not

difficult, and automated solid-phase synthesis is possible. Moreover, they have flexible sites for covalent attachment to other molecules. Hairpin polyamides linked with an alkylating agent may broaden the targets of transcriptional regulation of coding sequences [17]. In fact, we have successfully inhibited gene transcription of the green fluorescent protein and luciferase by alkylating hairpin polyamides [18].

Inhibiting the HIF transcription pathway is a fascinating strategy for cancer control, especially in the case of renal cell carcinomas. HIF controls genes related to the progression of cancers. Genes for platelet-derived growth factor (PDGF), VEGF, epidermal growth factor (EGF), and transforming growth factor-1α (TGF-1α are among those regulated by HIF-1 (a dimer of HIF-1α and ARNT). Therapeutic approaches using each of these molecules are being trialled clinically [19]. Avastin™ (anti-VEGF antibody), SU11248 (a small molecule targeting the tyrosine kinase domain of the VEGF receptor), and Tarceva™ or Iressa™ (molecules targeting the tyrosine kinase domain of the EGF receptor) are currently being investigated as potential agents against advanced renal cell carcinoma. Recently, we have shown that glucocorticoids can down-regulate VEGF in renal cell carcinoma cells [20]. Suppressing the binding of HIF-1 to the HRE may be a useful strategy for inhibition of these molecules. In addition, we and several other groups have demonstrated that HIF-2α, another α subunit of HIF, is more critical than HIF-1α in renal cell cancer [10,21]. As HIF-2 (a dimer of HIF-2α and ARNT) shares an HRE with HIF-1, targeting the HIF-HRE interaction may be more useful in the management of renal cell carcinoma than using the molecular therapeutic drugs described earlier. In the current study, the polyamide mixture successfully suppressed transcription induced not only by HIF-1α but also by HIF-2α. Our findings may facilitate the realization of the "transcription therapy" concept proposed by Dervan [5] for cancer treatment.

Conclusions

VEGF transcription was successfully suppressed by a combination of three Py-Im hairpin polyamides targeting the HRE. The use of Py-Im hairpin polyamides may be a new strategy for the treatment of renal cell carcinoma.

Acknowledgements

We thank Dr. Minori Koshiji and Ms. Kaoru Ito for their technical support. This work was supported by a Grant-in-Aid (14370505, 17591666, 17591667) for Scientific Research from the Ministry of Education, Science and Culture, Japan.

References

[1] Huang LE, Bunn HF. Hypoxia inducible factor and its biomedical relevance. J Biol Chem 2003;278:19575–8.
[2] Kaelin WG. The von Hippel-Lindau tumor suppressor gene and kidney cancer. Clin Cancer Res 2004;10:6290–5s.
[3] White S, Szewczyk JW, Turner JM, Baird EE, Dervan PB. Recognition of the four Watson-Crick base pairs in the DNA minor groove by synthetic ligands. Nature 1998;391:468–71.
[4] Murty MSRC, Sugiyama H. Biology of N-methylpyrrole-N-methylimidazole hairpin polyamide. Biol Pharm Bull 2004; 27:468–74.
[5] Dervan PB. Molecular recognition of DNA by small molecules. Bioorg Med Chem 2001;9:2215–35.
[6] Kielkopf CL, White S, Szewczyk JW, et al. A structural basis for recognition of A.T and T.A base pairs in the minor groove of B-DNA. Science 1998;282:111–5.
[7] Wang CC, Ellervik U, Dervan PB. Expanding the recognition of the minor groove of DNA by incorporation of beta-alanine in hairpin polyamides. Bioorg Med Chem 2001;9: 653–7.
[8] Ayame H, Saito T, Bando T, Fukuda N, Sugiyama H. Fmoc solid-phase synthesis and its application to pyrrole-imidazole polyamides. Nucleic Acids Res 2003;3:67–8s.
[9] Gnarra JR, Tory K, Weng Y, Schmidt L, Wei MH, Li H, et al. Mutations of the VHL tumor suppressor gene in renal carcinoma. Nature Genet 1994;7:85–90.
[10] Xia G, Kageyama Y, Hayashi T, Kawakami S, Yoshida M, Kihara K. Regulation of vascular endothelial growth factor transcription by endothelial PAS domain protein 1 (EPSA1) and possible involvement of EPAS1 in the angiogenesis of renal cell carcinoma. Cancer 2001;91:1429–36.
[11] Huang LE, Gu J, Schau M, Bunn HF. Regulation of hypoxia inducible factor 1α is mediated by an O2-dependent degradation domain via an ubiquitin-proteasome pathway. Proc Natl Acad Sci USA 1998;95:7978–92.
[12] Kageyama Y, Koshiji M, To KKW, Tian YM, Ratcliffe PJ, Huang LE. Leu-574 of human HIF-1a is a molecular determinant of prolyl hydroxylation. FASEB J 2004;18: 1028–30.
[13] Koshiji M, Kageyama Y, Pete EA, Horikawa I, Barret JC, Hunag LE. HIF-1α induces cell cycle arrest functionally counteracting Myc. EMBO J 2004;23:1949–56.
[14] Shibata T, Akiyama N, Noda M, Sasai K, Hiraoka M. Enhancement of gene expression under hypoxic conditions using fragments of the human vascular endothelial growth factor and the erythropoietin genes. Int J Radiat Oncol Biol Phys 1998;42:913–26.
[15] Takahashi R, Bando T, Sugiyama H. Specific alkylation of human telomere repeats by hairpin pyrrole-imidazole polyamide. Bioorg Med Chem 2003;11:2503–9.
[16] Olenyuk BZ, Zhang GJ, Klco JM, Nickols NG, Kaelin WG Jr, Dervan PB. Inhibition of vascular endothelial growth factor with a sequence-specific hypoxia response element antagonist. Proc Natl Acad Sci USA 2004;101: 16768–73.
[17] Oyoshi T, Kawakami W, Narita A, Bando T, Sugiyama H. Inhibition of transcription at a coding sequence by alkylating polyamide. J Am Chem Soc 2003;125:4752–4.

[18] Shinohara K, Narita A, Oyoshi T, Bando T, Teraoka H, Sugiyama H. Sequence-specific gene silencing in mammalian cells by alkylating pyrrole-imidazole polyamides. J Am Chem Soc 2004;126:5113–8.

[19] Linehan WM, Vasselli J, Srinivasan R, Walther MM, Merino M, Choyke P, et al. Genetic basis of cancer of the kidney: disease-specific approaches to therapy. Clin Cancer Res 2004;10:6282–9s.

[20] Iwai A, Fujii Y, Kawakami S, Takazawa R, Kageyama Y, Yoshida MA, et al. Down-regulation of vascular endothelial growth factor in renal cell carcinoma cells by glucocorticoids. Mol Cell Endocrinol 2004;226:11–7.

[21] Seagroves T, Johnson RS. Two HIFs may be better than one. Cancer Cell 2002;1:211–3.

0013-7227/06/$15.00/0
Printed in U.S.A.

Endocrinology 147(2):733–743

doi: 10.1210/en.2005-0679

Thioredoxin-Binding Protein-2-Like Inducible Membrane Protein Is a Novel Vitamin D3 and Peroxisome Proliferator-Activated Receptor (PPAR)γ Ligand Target Protein that Regulates PPARγ Signaling

Shin-ichi Oka, Hiroshi Masutani, Wenrui Liu, Hiroyuki Horita, Dongmei Wang, Shinae Kizaka-Kondoh, and Junji Yodoi

Institute for Virus Research (S.O., H.M., W.L., H.H., D.W., J.Y.), Kyoto University, Kyoto 606-8507, Japan; and Department of Therapeutic Radiology and Oncology (S.K.-K.), Kyoto University Graduate School of Medicine, Kyoto University, Yoshida-konoe-cho, Sakyo, Kyoto 606-8501, Japan

Thioredoxin binding protein-2 (TBP-2), which is identical with vitamin D3 (VD3) up-regulated protein 1 (VDUP1), plays a crucial role in the integration of glucose and lipid metabolism. There are three highly homologous genes of TBP-2/vitamin D3 up-regulated protein 1 in humans, but their functions remain unclear. Here we characterized a TBP-2 homolog, TBP-2-like inducible membrane protein (TLIMP). In contrast to TBP-2, TLIMP displayed no significant binding affinity for thioredoxin. TLIMP exhibited an inner membrane-associated pattern of distribution and also colocalized with transferrin and low-density lipoprotein, indicating endosome- and lysosome-associated functions. VD3 and ligands of peroxisome proliferator-activated receptor (PPAR)-γ, an important regulator of energy metabolism and cell growth inhibition, induced the expression of TLIMP as well as TBP-2. Overexpression of TLIMP suppressed both anchorage-dependent and -independent cell growth and PPARγ ligand-inducible gene activation. These results suggest that TLIMP, a novel VD3- or PPARγ ligand-inducible membrane-associated protein, plays a regulatory role in cell proliferation and PPARγ activation. (*Endocrinology* 147: 733–743, 2006)

IT IS WELL established that vitamin D3 (VD3) acts as a modulator of cell growth, differentiation, maintenance of extracellular calcium levels, bone mineralization, and lipid metabolism. VD3 exerts its actions through nuclear VD3 receptor (VDR)-mediated signal transduction and gene transcription (1). Another well-established nuclear receptor subfamily, peroxisome proliferator-activated receptors (PPARs), comprising PPARα, -δ (β), and -γ, binds fatty acids and play important roles in energy homeostasis. Thiazolidine derivatives, such as troglitazone and pioglitazone, which are selective PPARγ agonists, reduce hyperlipidemia in obese and diabetic animals (2–5). VDR and/or PPARs regulate gene transcription to modulate uptake of calcium, phosphate, lipids, and glucose from plasma (6, 7). In addition, several reports have suggested that VDR and PPARs have a regulatory role in the uptake of plasma proteins (8–11). However, the regulatory role and mechanisms of the membrane-associated function of VDR and PPARs largely remains to be clarified.

First Published Online November 3, 2005

Abbreviations: DTT, Dithiothreitol; EF, elongation factor; EGFP, enhanced green fluorescent protein; FABP4, fatty acid-binding protein 4; FCS, fetal calf serum; FITC, fluorescein isothiocyanate; GST, glutathione-S-transferase; LDL, low-density lipoprotein; LPL, lipoprotein lipase; PMA, phorbol 12-myristate 13-acetate; PPAR, peroxisome proliferator-activated receptor; RA, retinoic acid; TBP-2, thioredoxin binding protein-2; TLIMP, TBP-2-like inducible membrane protein; TRX, thioredoxin; VD3, vitamin D3; VDUP1, vitamin D3 up-regulated protein 1.

***Endocrinology* is published monthly by The Endocrine Society (http://www.endo-society.org), the foremost professional society serving the endocrine community.**

In the course of our study of thioredoxin (TRX), an important redox regulator (12, 13), we identified TRX-binding protein (TBP)-2 (14), which is identical with VD3 up-regulated protein 1 (VDUP1), a VD3-inducible gene in HL-60 cells (15). Several reports show that loss of TBP-2 expression is associated with cell growth or transformation. TBP-2 is down-regulated in human T cell leukemia virus I-transformed cells and human cancer tissues (16–19), whereas overexpression of TBP-2 induces cell growth suppression (18–20). Interestingly, HcB-19 mice, which have a nonsense mutation in the TBP-2 gene, exhibit hyperlipidemia characterized by elevated plasma triglyceride and/or cholesterol levels (21). The analyses of the HcB-19 mice (22) or TBP-2 knockout mice (23) revealed that TBP-2 plays a critical role in the integrated regulation of glucose and lipid metabolism in fasting. The molecular mechanisms underlying transformation and hyperlipidemia caused by loss of TBP-2 function remain to be elucidated, as does the mechanism behind the physiological function of TBP-2.

In this paper, we report that there are three homologous TBP-2/VDUP1 genes in humans. The TBP-2 homologs constitute a family and are preserved in *Schizosaccharomyces pombe*, *Saccharomyces cerevisiae*, *Drosophila melanogaster*, and *Caenorhabditis elegans* but not *Escherichia coli*, indicating that the genes have evolutionarily conserved roles in the eukaryotic system. However, the functions of these family members have not been clarified. Characterization of members of the human TBP-2 family will provide new insights into the biological roles of these genes. We have cloned a human TBP-2 homolog, TBP-2-like inducible membrane protein (TLIMP),

and show that TLIMP and TBP-2 are VD3/PPARγ ligand-inducible genes. To investigate the biological role of the TBP-2 gene family and understand the molecular mechanism of the VD3/PPAR-mediated cellular function, we characterized TLIMP and investigated the role of TLIMP in cellular growth regulation and PPARγ ligand-induced gene activation.

Materials and Methods

Reagents and materials

Phorbol 12-myristate 13-acetate (PMA), clofibrate, and prostaglandin J2 were purchased from Sigma (St. Louis, MO). Blasticidin was purchased from Kaken Pharmaceutical Co., Ltd. (Tokyo, Japan). Complete protease inhibitor cocktail was purchased from Roche Applied Science (Mannheim, Germany). Total RNAs from human cultured preadipocytes and adipocytes were purchased from Zen-Bio, Inc. (Research Triangle Park, NC). The human adipocytes were differentiated from preadipocytes by culturing with insulin and dexamethasone for 14 d. Troglitazone and pioglitazone were kindly provided by Sankyo Pharmaceutical Co. (Tokyo, Japan) and Takeda Pharmaceutical Co., Ltd. (Tokyo, Japan), respectively. L165,041 was purchased from Calbiochem (La Jolla, CA). Alexa-633-labeled transferrin, BODIPY FL-labeled low-density lipoprotein, fluorescein isothiocyanate (FITC)-conjugated anti-mouse IgG, Alexa 568-conjugated antimouse IgG, and LysoTracker Blue were purchased from Molecular Probes (Eugene, OR). Human 12-lane multiple tissue and cancer cell line Northern blots were obtained from CLONTECH (Mountain View, CA).

Amino acid sequence alignment

Amino acid sequences of TBP-2 family proteins were aligned using the ClustalW program (EMBL-European Bioinformatics Institute) and the BOXSHADE program (Swiss Institute of Bioinformatics) was used for formatting the results.

Plasmids

The open reading frame of TLIMP was amplified by PCR using the oligonucleotide primers 5′-AATGGATCCATGGTGCTGGGAAAGGTGAA-3′ and 5′-CGAATTCAACGAGAGGGGCAGGAT-3′. The cDNAs were subcloned into pCMV-Tag2B (CLONTECH) and pGEX6P1 (Amersham Biosciences, Piscataway, NJ) to generate pCMV-Flag-TLIMP and pGST-TLIMP, respectively. pEF-BSR, a blasticidin-resistant mammalian expression vector driven by the elongation factor (EF) 1 promoter, was kindly provided by Dr. Ishii (Riken Research Center for Allergy and Immunology, Yokohama, Japan). The cDNA containing a Kozak sequence in the 5′ side of the TLIMP gene lacking a stop codon was obtained by PCR using oligonucleotide primers 5′-GGAATTCGCCACCATGGTGCTGGGAAAGGT-3′ and 5′-CGGGATCCACGAGAGGGGCAGGATGGTCTA-3′. The TLIMP cDNA was ligated into pEF-BSR downstream of the EF promoter, and then a DNA fragment encoding the Flag epitope or enhanced green fluorescent protein (EGFP; pEGFP-N3; CLONTECH) was inserted into the 3′ end of TLIMP to generate pEF-BSR-TLIMP-Flag or pEF-BSR-TLIMP-EGFP, respectively. The N-terminal Flag epitope-tagged TBP-2 cDNA was ligated into pEF-BSR to generate pEF-BSR-Flag-TBP-2. Yeast expression vectors, pGBKT7-TLIMP and pGBKT7-TBP-2, for the expression of TLIMP or TBP-2 fused with the GAL4 DNA-binding domain were constructed by insertion of the open reading frames of TLIMP and TBP-2 into pGBKT7 (CLONTECH). The cDNA of TRX was ligated into pACT2 (CLONTECH) to generate pACT2-TRX, an expression vector for the GAL4 activation domain fused with TRX. Luciferase reporter plasmids containing five GAL4 binding sites in the promoter region (pGAL4-luc), and plasmid expressing PPARγ2 fused to the GAL4 DNA binding domain (pM-PPARγ2) and HA-tag (pcDNA3-HA-PPARγ2) were kindly provided by Dr. Ohshima (24).

Cell culture and transfection

HL-60 cells were cultured in RPMI 1640 medium. HeLa S3, COS7, and 293 cells were cultured in DMEM. CHO cells were cultured in F-12 medium. Heat-inactivated fetal calf serum (FCS) and antibiotics were added to the media. Cells were transfected with Lipofectamine (Invitrogen, Carlsbad, CA), according to the manufacturer's instructions. Stable transfectants were generated by transfection of HeLa S3 cells with either pEF-BSR-TLIMP-Flag or pEF-BSR control plasmid. After 24 h, cells were plated and selected in medium containing 4 μg/ml blasticidin. The expression of TLIMP in the transfectants was confirmed by Western blotting analyses. Reporter assay were performed as described previously (25). NIH3T3 cells were transfected with the TLIMP and GAL4-PPARγ2 expression vectors and luciferase reporter plasmids containing five GAL4 binding sites in the promoter region. Cells were then treated with troglitazone and luciferase reporter assay were performed (24).

Northern blotting analysis

Total RNA from cells was extracted using TRIzol reagent (Invitrogen), according to the manufacturer's instructions. Total RNA (10–20 μg/lane) was fractionated by denaturing agarose gel electrophoresis and transferred to a nylon membrane (Hybond N^+; Amersham Biosciences). The blots were hybridized with a [^{32}P]-labeled probe prepared using the BcaBest labeling kit (Takara, Shiga, Japan) overnight at 68 C.

Semiquantitative RT-PCR

Total RNAs from cells and tissues were extracted using TRIzol reagent (Invitrogen), according to the manufacturer's instructions. Reverse transcription was performed with a SuperScript III first-strand synthesis system kit (Invitrogen). PCRs were carried out using the following oligonucleotide primers: human TLIMP forward primer, 5′-ATGGTGCTGGGAAAGGTGAA-3′, and reverse primer, 5′-TCAACGAGAGGGGCAGGAT-3′; human TBP-2 forward primer, 5′-AAGGTGCTGACTCAGAAG-3′, and reverse primer, 5′-CTCACTGCACATTGTTGTTG-3′; human glyceraldehyde-3-phosphate dehydrogenase forward primer, 5′-ATGGGGAAGGTGAAGGTCGGAGTC-3′, and reverse primer, 5′-CCATGCCAGTGAGCTTCCCGTTC-3′; mouse TLIMP forward primer, 5′-ACAGTTACAGTGCCTGAGAAGACTCGG-3′, and reverse primer, 5′-GTGCCCTCAGGTGTTACGTCAAG-3′; mouse TBP-2 forward primer, 5′-GTGATGGATCTAGTGGATGTC-3′, and reverse primer, 5′-TCACTGCACGTTGTTGTTG-3′; mouse fatty acid-binding protein 4 (FABP4) forward primer, 5′-ACAAAATGTGTGATGCCTTTGTGGGAAC-3′, and reverse primer, 5′-TCCGACTGACTATTGTAGTGTTTGATGCAA-3′; mouse lipoprotein lipase (LPL) forward primer, 5′-GGGGTACCTGCCCACCACTTGTCCCCTGGAG-3′, and reverse primer, 5′-CGGGATCCCGGTGCACCCTTCTGCTTTGCTGC-3′; and mouse β-actin forward primer, 5′-ATGGATGACGATATCGCTGCGCT-3′, and reverse primer, 5′-TAGAAGCACTTGCGGTGCACGAT-3′. Amplification of the products is not saturated with the number of cycles performed.

Western blotting analysis

Cell lysates or immunoprecipitates were fractionated by SDS-PAGE and then transferred to a polyvinylidene difluoride membrane (Amersham Biosciences). Western blot analysis was performed using an enhanced chemiluminescence Western blotting detection system (Amersham Biosciences), according to the manufacturer's instructions.

Subcellular fractionation

Cells (at confluence in a 3.5 cm dish) were lysed with lysis buffer [25 mM Tris-HCl (pH 7.8), 2 mM dithiothreitol (DTT), 10% glycerol, 1% Trition X-100, and 1× complete protease inhibitor cocktail] and the cell lysate was centrifuged at 100,000 × *g* for 10 min. The supernatant, the Triton X-100 soluble fraction (100 μl) was transferred to a new tube, and 25 μl of 5× sample buffer [500 mM Tris-HCl (pH 6.8), 10% sodium dodecyl sulfate, 25% glycerol, 12.5% 2-mercaptoethanol, and 0.25% bromophenol blue] was added. The pellet, the Triton X-100 insoluble fraction, was resuspended with 125 μl of 1× sample buffer (5-fold dilution of 5× sample buffer with lysis buffer) before sonication. The fractionated samples were subjected to Western blotting analyses.

Immunofluorescent staining

Cells were cultured on glass-bottom dishes, fixed with 4% paraformaldehyde in PBS for 5 min at room temperature, and permeabilized for

5 min using 1% Nonidet P-40 in PBS. The permeabilized cells were incubated in PBS containing 1.5% FCS and then with anti-Flag antibody (Sigma) or anti-Myc antibody (Santa Cruz Biotechnology, Santa Cruz, CA), followed by FITC- or Alexa 568-conjugated antimouse IgG. The immunostained cells were examined with a confocal microscope (Leica Microsystems, Mannheim, Germany).

Preparation of recombinant proteins and in vitro binding assay

In vitro-translated proteins were prepared using a TNT-coupled rabbit reticulocyte translation system (Promega, Madison, WI). The [^{35}S]methionine-labeled translated products were analyzed by SDS-PAGE after performance of a glutathione-S-transferase (GST) pull-down assay. GST-TRX was prepared as described previously (14). The precipitates were detected by autoradiography using a Bio-image analyzer BAS2000 (Fuji Film Co. Ltd., Tokyo, Japan) or Coomassie Brilliant Blue staining.

Insulin-reducing assay

COS7 cells were transiently transfected with the GFP-TBP-2 or TLIMP expression vector. After 3 d, the cells (at confluence in a 10 cm dish) were collected and lysed by the freeze and thaw method. The cell lysate (10 mg/ml, 10 μl) was preincubated with 2.5 μl DTT activation buffer [0.1 M Tris-HCl (pH 7.5), 2 mM EDTA, 1 mg/ml BSA, and 2 μM DTT] for 15 min at 37 C. The preincubated samples were mixed with 110 μl reaction buffer [0.1 M Tris-HCl (pH 7.5), 2 mM EDTA, 0.2 mM nicotinamide adenine dinucleotide phosphate reduced, and 0.4 U/ml yeast TRX reductase], and then 10 μl insulin solution [50 mM Tris-HCl (pH 7.5), 10 mg/ml insulin] were added to the mixture. The decrease in nicotinamide adenine dinucleotide phosphate reduced absorbance at 340 nm was recorded (maximal velocity, millioptical density at 340 nm/min) at room temperature. The calculated values were compared with the standard curve for recombinant TRX to obtain a quantitative determination of the absolute amounts of TRX.

Yeast two-hybrid analysis

The yeast two-hybrid analysis was performed using the yeast MATCHMAKER two-hybrid system (CLONTECH), according to the manufacturer's directions. *S. cerevisiae* strain AH109 transformed with pGBKT7-TLIMP or pGBKT7-TBP-2, together with either pACT2 or pACT2-TRX, respectively. Transformed colonies were cultured in synthetic medium with or without histidine.

Cell proliferation assay

Blasticidin-resistant mammalian expression vectors were introduced into CHO cells, and the cells were cultured with 8 μg/ml of blasticidin-containing medium for 2 or 3 d to eliminate the nonresistant cells. The blasticidin-resistant cells (3–5 × 10^3 cells in 100 μl of culture medium containing 8 μg/ml of blasticidin) were cultured in 96-well flat-bottom microtiter plates. Cell proliferation was measured as the formation of formazan using SF cell-counting reagents (Nacalai Tesque, Kyoto, Japan), according to the manufacturer's instructions.

Colony formation assay

Blasticidin-resistant mammalian expression vectors were introduced into HeLa S3 cells, and the cells were cultured with 4 μg/ml of blasticidin-containing medium for 3 d. The cells (1 × 10^6 cells) were plated in 0.35% agar containing DMEM, 10% FCS, and 4 μg/ml of blasticidin on a 0.5% agar base layer containing DMEM. The total number of foci was scored after 10 d.

Statistical methods

Results are expressed as means ± SD. Statistical comparisons were made using Student's *t* test or ANOVA coupled with a Fisher's test. A statistically significant difference was defined as $P < 0.05$, which is represented by an *asterisk* in the data presentation.

Results

TBP-2 protein family

As shown in Fig. 1A, BLAST searches were used to identify human genes homologous to TBP-2. DRH1 and two other genes (GenBank accession no. AF193051 and BC015928) were identified. DRH1 has been reported as a gene that is down-regulated in advanced human hepatocellular carcinoma (26). Here we refer to BC015928 as TLIMP, which was originally identified as KIAA1376 when it was found in the full-length human cDNA sequencing project (27). The function of AF193051 has not been reported. TLIMP has 40% identity and over 80% similarity with TBP-2 at the amino acid level, and the other genes also exhibit high levels of identity and similarity. All the genes included eight exons, each of which encodes a corresponding region of the protein (Fig. 1B and supplemental Fig. 1, published as supplemental data on The Endocrine Society's Journals Online web site at http://endo.endojournals.org). Therefore, it is likely that this mammalian gene family was generated by gene duplications. The members of the TBP-2 gene family also have some homology to arrestin proteins. For example, TLIMP has 25% similarity with β-arrestin-1 at the amino acid level. TBP-2 and arrestins have similar numbers of amino acids (~400) and show overall similarity, rather than just a highly conserved region.

TLIMP cDNA was cloned from a 293-cell cDNA library by PCR and then sequenced. Two isoforms of TLIMP cDNA with different lengths were found (Fig. 1C). The longer cDNA encoded full-length TLIMP, producing a protein of 414 amino acids. The shorter TLIMP splice variant, referred to as TLIMPs, lacks 148 bp corresponding to exon 3, generating a 24-amino-acid C-terminal tail and a translational stop codon and producing a shorter protein of 144 amino acids (Fig. 1D).

Tissue distribution of TLIMP expression

The expression of TLIMP was analyzed in normal human tissues and human cancer cell lines, and as shown in Fig. 2A, the size of TLIMP mRNA was about 4.5 kb in both normal and cancer cells. Strong expression of TLIMP was detected in normal skeletal muscle, placenta, kidney, adrenal gland, lymph node, mammary gland, thyroid, and trachea, but only very weak expression was detected in normal colon, thymus, spleen, small intestine, bladder, and bone marrow. In human cancer cell lines, TLIMP was strongly expressed in the lung adenocarcinoma cell line A549, whereas low expression levels were observed in other cancer cell lines. The expression of TBP-2 was strong in normal heart, skeletal muscle, spleen, and peripheral blood lymphocytes, and weak in normal brain and liver (Fig. 2B). The distribution of TLIMP was clearly different from that of TBP-2 in some tissues.

TLIMP does not interact with TRX

TBP-2 binds to TRX *in vivo* and *in vitro* (14), but no interaction of TLIMP with TRX was detected in a yeast two-hybrid analysis, as shown in Fig. 3A. The same analysis showed binding of TRX with TBP-2. Similar results were obtained in *in vitro* binding assays, in which TBP-2 coprecipitated with GST-TRX, but TLIMP failed to do so (Fig. 3B). Overexpres-

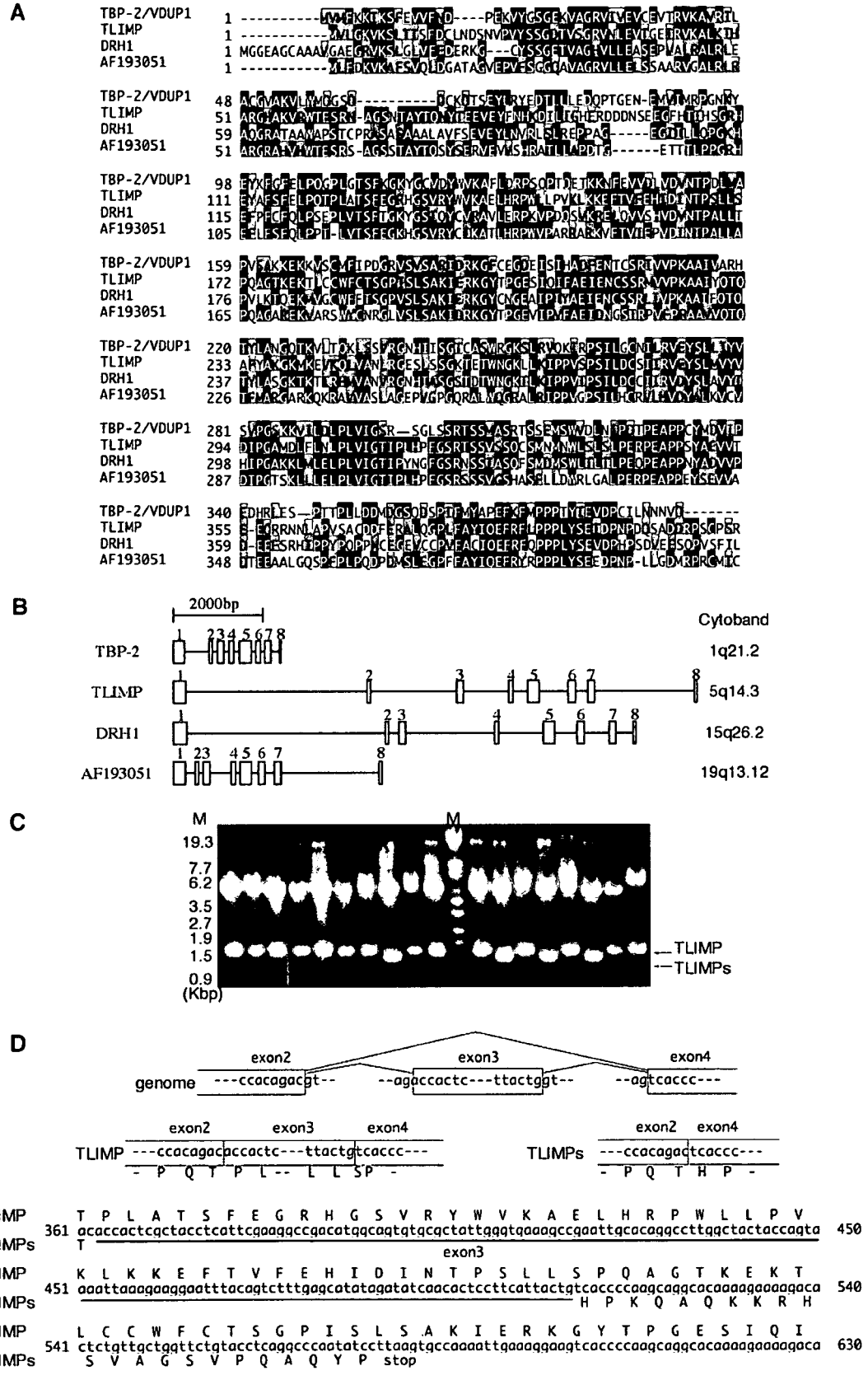

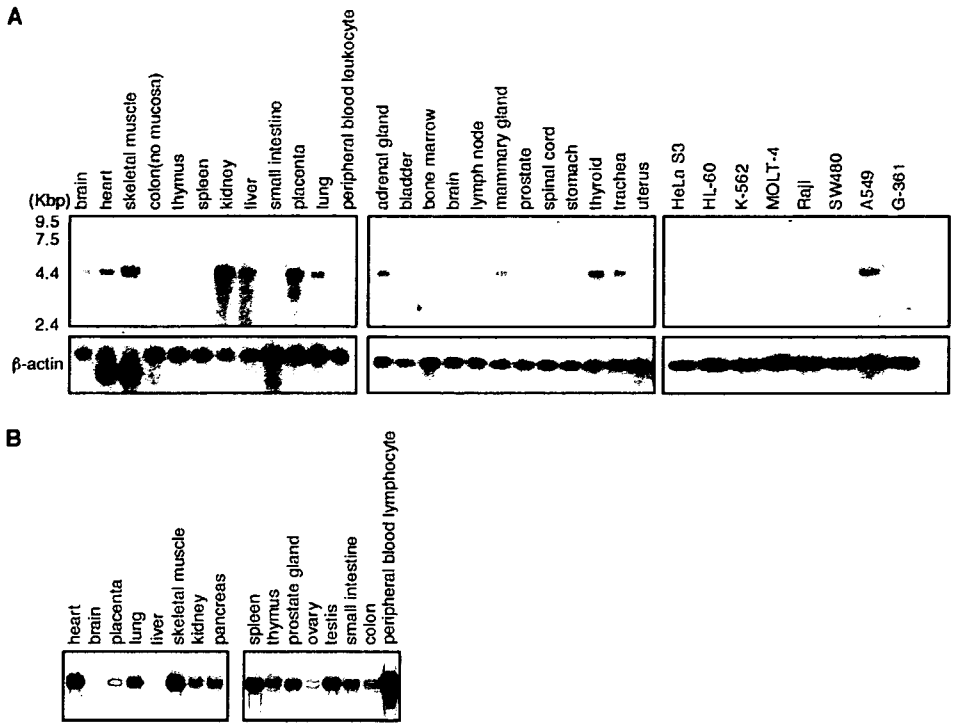

FIG. 2. Analysis of TLIMP expression: tissue distribution of TLIMP (A) and TBP-2 (B). RNA blots containing poly (A)+ RNA from multiple human tissues or cancer cell lines were hybridized with full-length TLIMP or TBP-2 cDNA as a probe. Human β-actin was used as a control to determine the relative amount of RNA from each of the tissues or cells.

sion of TBP-2 has been shown to suppress the reducing activity of TRX (14), and the effect of TLIMP on this activity was examined in an insulin-reducing assay. TRX-reducing activity was not significantly changed in cellular extracts transiently expressing TLIMP, whereas it was significantly suppressed in cellular extracts transfected with TBP-2 (Fig. 3C). These results indicate that TRX interacts with TBP-2 but not with TLIMP.

Intracellular localization of TLIMP

To determine the intracellular distribution of TLIMP, Flag-tagged TLIMP (TLIMP-Flag) was expressed in HeLa S3, 293, COS7, and CHO cells. The cellular distribution of TLIMP-Flag is shown in Fig. 4A. Immunofluorescent analysis using anti-Flag antibody showed that TLIMP is present in the plasma membrane and small vesicular structures scattered throughout the cytoplasm. As reported previously, TBP-2 was detected mainly in the nucleus and partly in the cytoplasm in COS7 cells (19). To determine whether TLIMP is expressed on the inner or outer side of the plasma membrane, TLIMP-Flag was expressed in HeLa S3 cells and stained by Nonidet P-40 without permeabilization. TLIMP-Flag was not stained in the nonpermeabilized cells but significantly stained in the permeabilized cells, indicating that TLIMP is expressed on the inner side of the plasma membrane (Fig. 4B). The vesicular pattern of TLIMP protein expression in cytoplasm is similar to that of endosomes or lysosomes. To analyze whether TLIMP is present in the cellular compartments, we examined the distribution of EGFP-tagged TLIMP with Alexa633-conjugated transferrin and LysoTracker Blue, which are markers for endosomes and lysosomes, respectively. As shown in Fig. 4C, TLIMP-EGFP showed a similar distribution to TLIMP-Flag, and the fluorescence merged with that of transferrin or LysoTracker in intracellular vesicular structures. Merging of all three fluorescent signals was observed in several areas. Whereas internalized transferrin is predominantly recycled to the plasma membrane through recycling of endosomes, low-density lipoprotein (LDL) is internalized and transported into lysosomes. To validate whether TLIMP is present in the lysosomal pathway, the cellular localizations of TLIMP and LDL were examined. As shown in Fig. 4D, the fluorescence of internalized LDL partly merged with TLIMP. These results suggest that TLIMP expression is associated with the plasma membrane, endosomes, and lysosomes during endocytosis.

FIG. 1. The TBP-2 protein family. A, ClustalW alignment of the amino acid sequences of the human TBP-2 family. The numbers on the *left* refer to the amino acids of each protein. B, Intron-exon structures of the TBP-2 gene family. The coding exons of the proteins are depicted as *boxes*. *Upper numbers* indicate the order of each exon. The *signatures on the right* indicate the cytoband of each protein. The *scale below* defines the proportional length of the genomic sequences. C, Alternatively spliced form of TLIMP. The amplified cDNA of TLIMP was subcloned into pCMV-Tag2 (Stratagene, La Jolla, CA) and the length of the insert was checked by restriction enzyme (*Hin*dIII) digestion. A DNA marker is shown in lane M. D, Summary of the two spliced isoforms. The shorter isoform, TLIMPs, lacks 148 bp corresponding to exon 3 (*underlined*), with a translational stop codon after a short 24-amino-acid C-terminal tail.

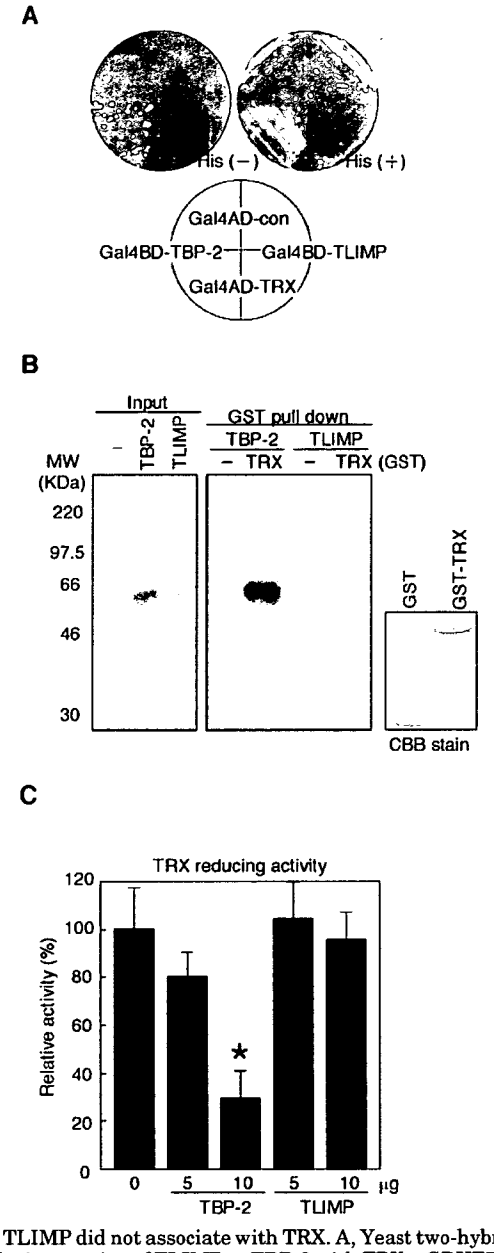

FIG. 3. TLIMP did not associate with TRX. A, Yeast two-hybrid analysis of the interaction of TLIMP or TBP-2 with TRX. pGBKT7-TLIMP or pGBKT7-TBP-2 was introduced into the yeast strain AH109 with either pACT2 or pACT2-TRX. The growth of the yeast transformants on a selective synthetic medium with or without histidine is shown. B, GST pull-down analysis of the interaction of TLIMP or TBP-2 with TRX. ^{35}S-labeled TLIMP or TBP-2 precipitated with GST-TRX or GST immobilized on GSH beads. The *right panel* shows that equal amounts of GST-fusion proteins were used in the pull-down assay, as determined by Coomassie Brilliant Blue staining. C, The effect of TRX activity on TLIMP expression. The TRX activity of the extract of COS7 cells transiently transfected with the indicated amount of expression vector for GFP-TBP-2 or GFP-TLIMP fusion proteins was determined in an insulin reducing assay. Expression vectors (10 μg/plate) were introduced into cells cultured in 10-cm dishes. The total DNA concentration was kept constant using pEGFP-C1. Activities of samples are shown relative to the control value (lane 1), which is taken as 100%. The results are shown as the mean ± SD of three samples.

Regulation of TLIMP expression

Because TBP-2 was first identified as a gene, the expression of which was induced by VD3 in HL-60 cells, TLIMP expression in VD3-treated HL-60 cells was examined. Expression of TLIMP was also induced when HL-60 cells were cultured in the presence of VD3, in a time- and dose-dependent manner (Fig. 5A). The effects of retinoic acid (RA) and PMA on the expression of TBP-2 and TLIMP were then tested. RA and PMA are known to induce differentiation of HL-60 cells into granulocytes and macrophage-like cells, respectively. As shown in Fig. 5B, specific morphological changes in HL-60 cells were observed on treatment with RA, VD3, and PMA. RA did not induce TBP-2 or TLIMP expression, whereas PMA significantly induced the expression of TLIMP but not TBP-2. The extent of induction of TLIMP expression by PMA was less than that by VD3. TRX expression decreased in cells treated with VD3, RA, and PMA.

PPARγ has been implicated in the regulation of cell growth and differentiation of cells or tissues, such as adipose tissues, breast, and colon (28). Similarly to VD3, PPAR ligands induce monocytic differentiation and concomitantly inhibit cell proliferation in HL-60 cells (29, 30). These findings led us to hypothesize that members of the TBP-2 family have a role in the biological responses elicited by not only VD3 but also PPAR ligands. Therefore, the effects of PPAR ligands on the expression of TBP-2 and TLIMP were examined in HL-60 cells. Troglitazone, a selective PPARγ agonist, significantly induced both TBP-2 and TLIMP expression in a time- and dose-dependent manner (Fig. 5C). These genes were also up-regulated by pioglitazone, another PPARγ agonist. Clofibrate, a selective PPARα agonist, markedly induced TBP-2 expression but had no effect on TLIMP expression. These results suggest that TBP-2 and TLIMP are both up-regulated by PPARγ ligands but differentially regulated by PPARα ligands. TRX expression was decreased with all the PPAR agonists tested, showing a reciprocal pattern to TBP-2 expression (Fig. 5D). To further study the effect of PPAR ligands on the expression of these genes, we examined the effects of L165,041, a PPARβ/δ ligand, and prostaglandin J2, an endogenous ligand of PPARγ, on the levels of TLIMP and TBP-2 expression (31). As shown in Fig. 5E, both TLIMP and TBP-2 are up-regulated by prostaglandin J2 but not L165,041. Collectively, the above results indicate that both TLIMP and TBP-2 are downstream regulatory proteins of VD3 and PPARγ.

Because PPARγ plays an important role in differentiation in adipocytes as well as monocytes, the expression levels of TLIMP and TBP-2 were examined during differentiation of adipocytes *in vitro*. As shown in Fig. 6, both TLIMP and TBP-2 are strongly expressed in adipocytes, compared with preadipocytes, indicating that these genes are up-regulated in association with differentiation of adipocytes. Expression of TLIMP and TBP-2 was also detected in brown and white adipose tissues *in vivo* (Fig. 6B), and collectively these results suggest that both TLIMP and TBP-2 play a role in the differentiation and function of adipocytes.

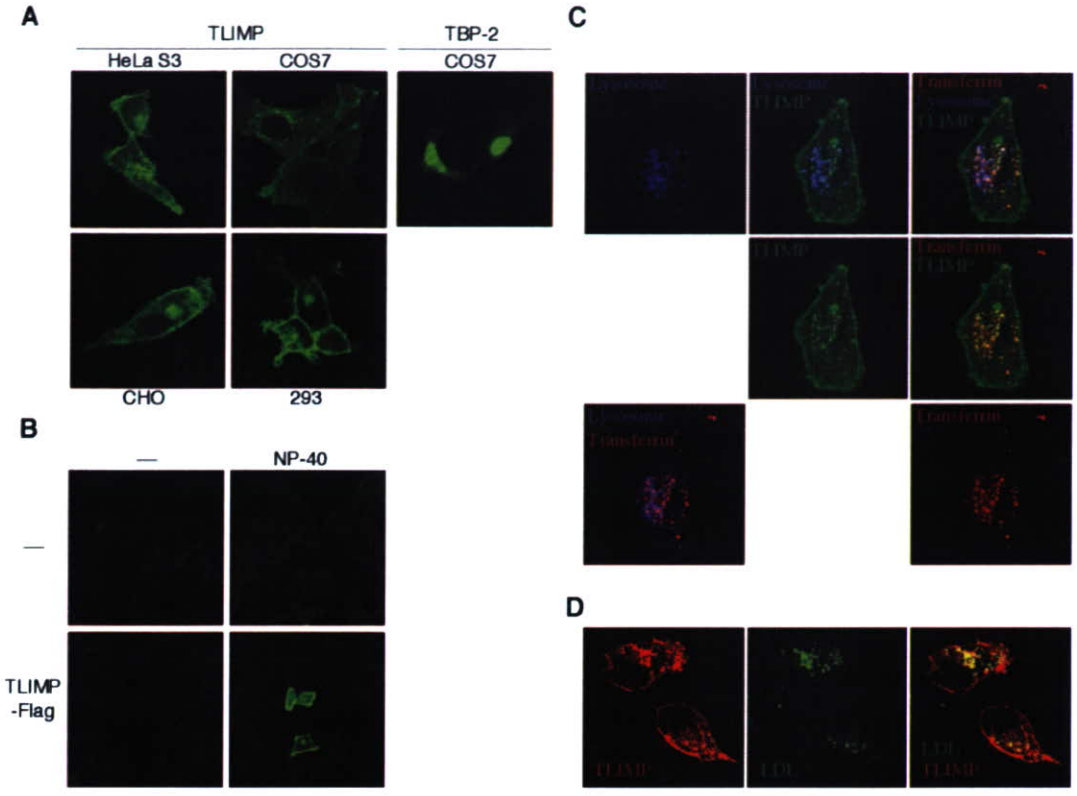

FIG. 4. Cellular localization of TLIMP. A, Expression of TLIMP. Flag epitope-tagged TLIMP was transiently expressed in HeLa S3, 293, COS7, and CHO cells. C-terminal Myc epitope-tagged TBP-2 was transiently expressed in COS7 cells. The cells were permeabilized by 1% Nonidet P-40 and then immunostained using anti-Flag or anti-Myc antibody, and FITC-conjugated antimouse IgG, as described in *Materials and Methods*. B, Detection of TLIMP protein in permeabilized cells. HeLa S3 cells transfected with TLIMP-Flag were immunostained after permeabilization with 1% Nonidet P-40 or after no permeabilization. A and B, The fixed and immunostained cells were analyzed using confocal microscopy. C, Colocalization of TLIMP, transferrin, and LysoTracker. HeLa S3 cells expressing C-terminal EGFP-tagged TLIMP were incubated with 50 nM LysoTracker Blue for 1 h and then 20 μg/ml Alexa633-labeled transferrin for 15 min. All combinations of merged colors are indicated. D, Colocalization of TLIMP and LDL. HeLa S3 cells expressing C-terminal Flag-tagged TLIMP were incubated with 50 μg/ml BODIPY FL-labeled LDL for 1 h and then immunostained using anti-Flag antibody and Alexa 568-conjugated antimouse IgG, as described in *Materials and Methods*. Merged colors are indicated.

Suppression of cell growth by TLIMP

VD3 and PPAR ligands are known to have strong cell growth-inhibitory activity in HL-60 cells, and previous reports have shown that TBP-2 also inhibits cell proliferation (18, 19). To investigate whether TLIMP also has this inhibitory activity, the effect of overexpression of TLIMP on cell proliferation was examined. In TLIMP transfectants, TLIMP was mainly detected in the Triton X-100-insoluble fraction (Fig. 7A, *upper panel*), indicating that the majority of TLIMP was localized in the detergent-insoluble membrane fraction. CHO cells transiently overexpressing TLIMP showed retardation of cell growth (Fig. 7A). It has been reported that TBP-2 suppresses anchorage-dependent and anchorage-independent cell growth (32), and to test the role of TLIMP in anchorage-independent cell growth, the growth of TLIMP-overproducing HeLa S3 cells was examined in culture in a semisolid medium. The number and size of foci was reduced in TLIMP- and TBP-2-transfected cells (Fig. 7B). These results demonstrate that both TLIMP and TBP-2 suppress anchorage-dependent and -independent cell growth.

TLIMP suppresses ligand-induced PPARγ activation

We next hypothesized that up-regulation of TLIMP by PPARγ ligands plays a role in PPARγ signaling through feedback regulation. To test this hypothesis, we analyzed the effect of overexpression of TLIMP on PPARγ transactivation in NIH3T3 cells, with a reporter assay using a GAL4-fused PPARγ2 expression vector and a luciferase reporter plasmid containing GAL4 binding sites in the promoter region. As shown in Fig. 8, troglitazone-induced reporter activation was suppressed by overexpression of TLIMP, suggesting that TLIMP negatively regulates ligand-induced PPARγ activation.

PPARs induce the expression of responsive target genes such as FABP4 and LPL through direct binding to the peroxisome proliferator-responsive element in their promoter regions (33, 34). To investigate the effect of TLIMP on PPARγ-induced endogenous gene expression, the levels of FABP4, LPL, TLIMP, and TBP-2 were examined in cells overexpressing PPARγ and TLIMP. As shown in Fig. 8B, expression of the target genes in cells expressing PPARγ increased with treatment with troglitazone. The induction of expression was

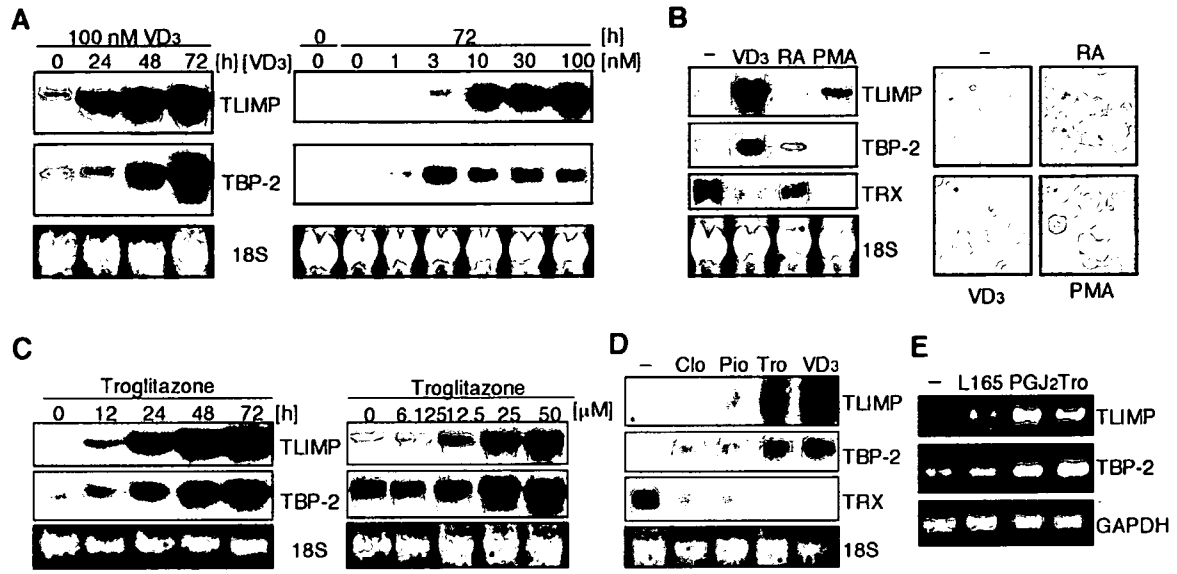

FIG. 5. The effect of inducers of differentiation on TLIMP expression. A, Expression of TLIMP and TBP-2 in VD3-stimulated HL-60 cells. At the indicated time points, total RNA was isolated from cells treated with 100 nM (*left*) or various concentrations (*right*) of VD3. B, Expression of TLIMP, TBP-2, and TRX in HL-60 cells treated with VD3, RA, PMA. Cells were cultured with 100 nM VD3, 10 μM RA, and 100 ng/ml of PMA for 76 h. Morphological changes of the HL-60 cells are shown in the photographs on the *right*. C, Expression of TLIMP and TBP-2 in troglitazone-stimulated HL-60 cells. At the indicated time points, total RNA was isolated from cells treated with 50 μM (*upper*) or various concentrations (*lower*) of troglitazone for 72 h. D, Expression of TLIMP, TBP-2, and TRX in HL-60 cells treated with troglitazone, pioglitazone, and clofibrate. Cells were cultured with 100 μM clofibrate (Clo), 50 μM pioglitazone (Pio), 50 μM troglitazone (Tro), and 100 nM VD3 for 72 h. The isolated total RNA (20 μg/lane) was fractionated and transferred to a nylon membrane, as described in *Materials and Methods*. The same membrane was hybridized with a [^{32}P]-labeled probe using cDNA encoding TLIMP, TBP-2, or TRX. E, Expression of TLIMP and TBP-2 in HL-60 cells treated with L165,041 and prostaglandin J2. Cells were cultured with 10 μM L165,041 (L165), 10 μM prostaglandin J2 (PGJ2), or 50 μM troglitazone (Tro) for 72 h. The expression levels of TLIMP and TBP-2 were determined by RT-PCR using cDNA prepared using RNA from the cells.

suppressed by overexpression of TLIMP, suggesting that TLIMP negatively regulates PPARγ-dependent gene activation.

Discussion

In the present study, we found that there are four familial TBP-2 genes, TBP-2/VDUP1, TLIMP, AF193051, and DRH1 in humans. Members of the human TBP-2 protein family share some common features but also have different features. TBP-2 and AF193051 were predominantly concentrated in the nucleus (20) (Tan, A., S. Oka, M. Mochizuki, H. Masutani, and J. Yodoi, unpublished observation), whereas TLIMP was found in the plasma membrane, lysosomes, and endosomes. The cellular distribution of DRH1 is similar to that of TLIMP; EGFP-tagged DRH1 has been found to be predominantly distributed in small vesicular structures at the periphery of the nucleus in COS7 cells (26), suggesting the localization in endosomes and/or lysosomes. TBP-2 familial proteins may coordinately regulate common cellular functions in different subcellular compartments. TBP-2 proteins have remote homology to the arrestin family of proteins, which play an important role in the internalization of G protein-coupled receptors and transforming growth factor-β, thereby quenching their signal transduction (35, 36). Based on the structural homology, TLIMP may have a similar biological role such as protein trafficking during endocytosis as well as scaffold or adaptor function similar to arrestin (37). Indeed, overexpression of TLIMP suppressed the uptake of transferrin (data not shown). It could be also postulated that TLIMP itself is associated with endocytosis of VD3 or endogenous ligands of PPARγ.

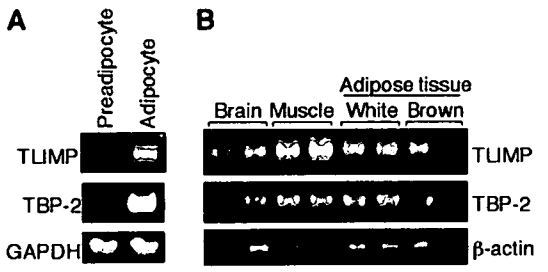

FIG. 6. Expression of TLIMP and TBP-2 in adipose cells and tissues. A, Expression of TLIMP and TBP-2 in association with differentiation of adipocytes. The expression levels of TLIMP and TBP-2 were determined by RT-PCR using cDNA prepared using RNA from human adipocytes and preadipocytes. B, Expression of TLIMP and TBP-2 in brown and white adipose tissues *in vivo*. RT-PCR was performed using cDNA prepared using RNA from the indicated tissues in C57BL/6 mice.

Expression levels of TLIMP and TBP-2 were significantly up-regulated by VD3 and PPARγ agonists, rather than by RA and PMA, in HL-60 cells (Fig. 5). These results indicate that the induction of TLIMP and TBP-2 expression in HL-60 cells is specifically associated with differentiation of monocytes and not with granulocytes. In addition, TLIMP and TBP-2 were up-regulated in association with differentiation of adipocytes (Fig. 6), indicating that these genes play an important role in PPARγ-mediated adipogenesis or lipid metabolism.

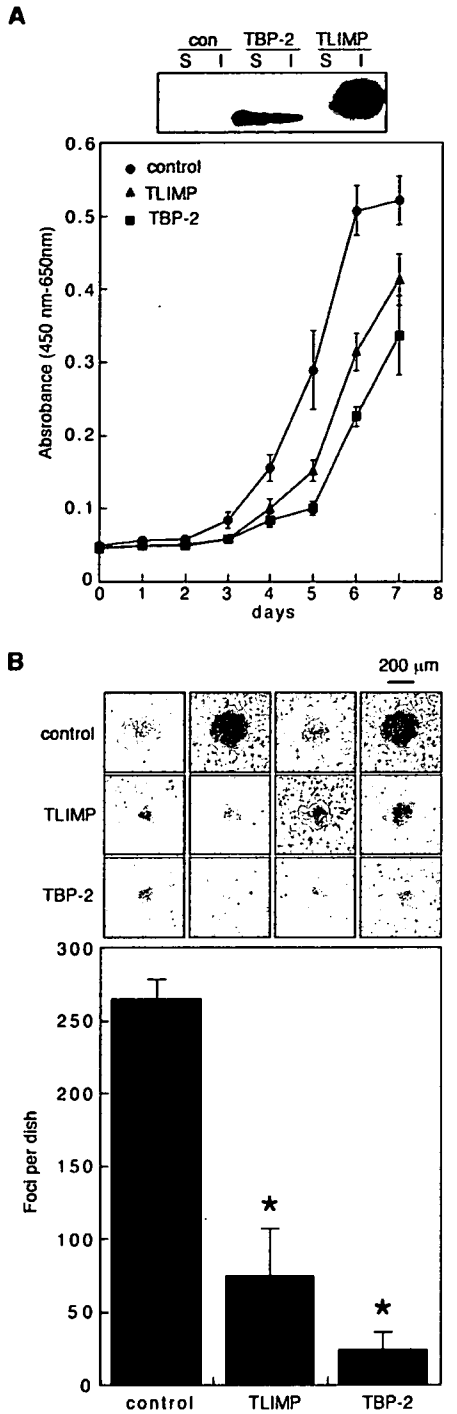

FIG. 7. Cell growth suppressive effect of TLIMP. A, Suppression of cell proliferation by TBP-2 and TLIMP. The cell proliferation rate was analyzed in CHO cells transiently transfected with pEF-BSR, pEF-BSR-TBP-2-Flag, or pEF-BSR-TLIMP-Flag vectors. B, Suppression of anchorage-independent cell proliferation by TBP-2 and TLIMP. Blasticidin-resistant expression vectors, pEF-BSR, pEF-BSR-TBP-2-Flag, and pEF-BSR-TLIMP-Flag, were used to transiently transfect HeLa S3 cells. A colony formation assay was performed as described in *Materials and Methods*. The results are shown as the mean ± SD of triplicate cultures. Foci are shown in the *upper photographs*.

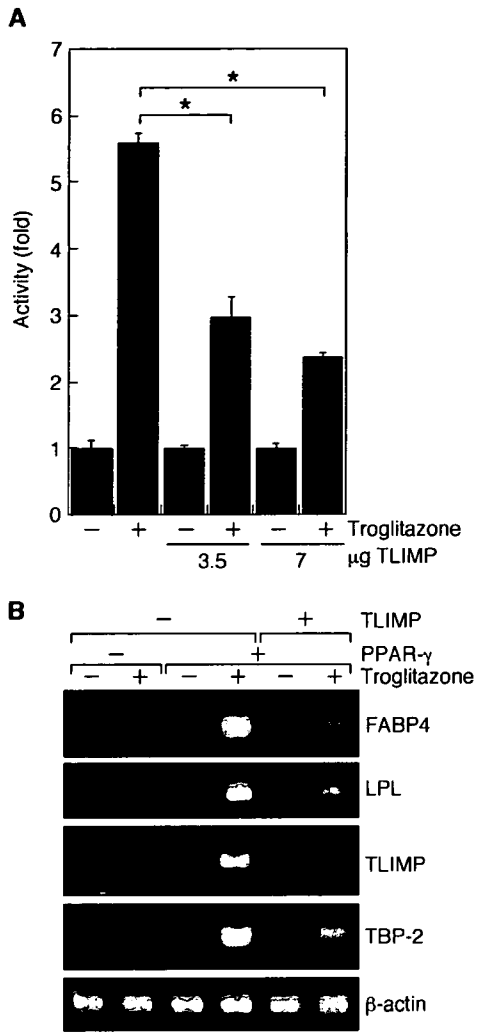

FIG. 8. TLIMP suppresses troglitazone-induced PPARγ activation. A, PPARγ-dependent transactivation is suppressed by overexpression of TLIMP. NIH3T3 cells were cotransfected with 1 μg pGAL4-luciferase reporter plasmid (pGAL4-luc) and 2 μg of plasmid expressing PPARγ2 fused to the GAL4 DNA binding domain (pM-PPARγ2) with or without the indicated amount of Flag-tagged TLIMP expression plasmid (pEF-BSR-TLIMP-Flag). Twenty-four hours after transfection, cells were treated with 10 μM troglitazone and cultured for 18 h. Luciferase activities were then measured. B, TLIMP inhibits PPARγ-dependent gene expression. NIH3T3 cells were transfected with 2 μg HA-tagged expression plasmid (pcDNA3-HA-PPARγ2) with or without 2 μg of Flag-tagged TLIMP expression plasmid (pEF-BSR-TLIMP-Flag). Twenty-four hours after transfection, the cells were treated with 10 μM troglitazone and cultured for 18 h. The expression levels of the indicated genes were determined by RT-PCR.

The promoter regions of the TLIMP and TBP-2 genes do not have a classical VDR or PPAR response element. The mechanism of the regulations should be further investigated.

We have several pieces of evidence that the expressions of TBP-2 familial genes are differentially regulated. VD3 and PPARγ agonists failed to induce the expression of both AF193051 and DRH1 in HL-60 cells (data not shown). In addition, suberoylanilide hydroxamic acid, a histone deacetylase

inhibitor, induced expression of TBP-2 expression but not TLIMP in HeLa S3 cells (supplemental Fig. 2, published as supplemental data on The Endocrine Society's Journals Online web site at http://endo.endojournals.org), although a nuclear factor-Y-binding site is conserved in the TLIMP and TBP-2 promoter regions. It is reported that suberoylanilide hydroxamic acid induces the expression of TBP-2 through activation of nuclear factor-Y (17).

TLIMP and TBP-2 suppressed both anchorage-dependent and -independent cell proliferation (Fig. 7). These activities may contribute to the growth-suppressive effects of VD3 and PPAR agonists, which also inhibit anchorage-dependent and -independent cell growth (38, 39).

The mechanism of TLIMP-induced growth inhibition is currently unclear. Inhibition of the TRX-reducing activity or an effect on the nuclear compartment has been suggested as a mechanism of TBP-2-induced cell growth inhibition (20, 40). However, it is unlikely that TLIMP suppresses cell growth through inhibition of TRX-reducing activity because it failed to bind to TRX or inhibit its reducing activity (Fig. 3). There are many important cell growth-regulating molecules including receptor tyrosine kinases, nonreceptor tyrosine kinases, and (small) G-proteins in the plasma membrane, whose endocytosis leads to a quenching of the signal transduction elicited by the molecules (41). VD3 modulates signal transduction proximal to the plasma membrane for phospholipase C, protein kinase C, and calcium channels (1). In addition, it is reported that 15-deoxy-Δ-12, 14-prostaglandin J2, a natural ligand for PPARγ, prevents cell proliferation through inhibition of ErbBs, a receptor tyrosine kinase family (42). It is possible that TLIMP suppresses cell growth through the modulation of signal transduction in the plasma membrane and/or endosomes. On the other hand, TLIMP suppresses ligand-induced PPARγ activation (Fig. 8), suggesting the negative feedback loop between TLIMP and PPARγ. In addition to ligand binding, PPARγ activity is modulated by MAPK through direct phosphorylation (43). TLIMP may modulate the activity of PPARγ through the regulation of up-stream signaling of these kinases in proximal plasma membrane. The mechanism of the effect of TLIMP in cell proliferation and PPARγ activation requires further study.

In conclusion, we have shown that TLIMP, a VD3 or PPARγ target protein, regulates cell proliferation and PPARγ activation. The cellular localization associated with endocytotic membrane trafficking suggests that TLIMP is a molecule connecting the PPARγ signal and endosomal functions, providing a novel mechanism of regulation by VD3 or PPARγ signals .

Acknowledgments

We thank Drs. Kimishige Ishizaka, Toshiro Tsukamoto, Yasuyuki Ishii, and Takayuki Ohshima and Hajime Nakamura and Yoshihiro Ohmiya for helpful discussions; Ms. Yoko Kanekiyo for secretarial help; Drs. Masaki Tanito and Yong-Chul Kim for technical help; and Drs. Kenji Kasuno and Kaimul Md. Ahsan for generously providing some of the experimental materials.

Received June 6, 2005. Accepted October 25, 2005.

Address all correspondence and requests for reprints to: Hiroshi Masutani, Department of Biological Responses, Institute for Virus Research, Kyoto University, 53 Kawahara-cho, Shogoin, Sakyo, Kyoto 606-8507, Japan. E-mail: hmasutan@virus.kyoto-u.ac.jp.

This work was supported by a grant-in-aid for Scientific Research from the Ministry of Education, Culture, Sports, Science, and Technology of Japan and the Research and Development Program for New Bio-Industry Initiatives. S.O. was supported by the New Energy and Industrial Technology Development Organization Fellowship Program. W.L. is a postdoctoral fellowship and recipient of a grant-in-aid from the Japan Society for the promotion of Science. D.W. has been supported by the 21st Century Centers of Excellence Program of the Ministry of Education, Culture, Sports, Science, and Technology of Japan.

References

1. **Norman AW, Okamura WH, Bishop JE, Henry HL** 2002 Update on biological actions of 1α,25(OH)2-vitamin D3 (rapid effects) and 24R,25(OH)2-vitamin D3. Mol Cell Endocrinol 197:1–13
2. **Barak Y, Nelson MC, Ong ES, Jones YZ, Ruiz-Lozano P, Chien KR, Koder A, Evans RM** 1999 PPAR gamma is required for placental, cardiac, and adipose tissue development. Mol Cell 4:585–595
3. **Dreyer C, Keller H, Mahfoudi A, Laudet V, Krey G, Wahli W** 1993 Positive regulation of the peroxisomal β-oxidation pathway by fatty acids through activation of peroxisome proliferator-activated receptors (PPAR). Biol Cell 77:67–76
4. **Peters JM, Hennuyer N, Staels B, Fruchart JC, Fievet C, Gonzalez FJ, Auwerx J** 1997 Alterations in lipoprotein metabolism in peroxisome proliferator-activated receptor α-deficient mice. J Biol Chem 272:27307–27312
5. **Kubota N, Terauchi Y, Miki H, Tamemoto H, Yamauchi T, Komeda K, Satoh S, Nakano R, Ishii C, Sugiyama T, Eto K, Tsubamoto Y, Okuno A, Murakami K, Sekihara H, Hasegawa G, Naito M, Toyoshima Y, Tanaka S, Shiota K, Kitamura T, Fujita T, Ezaki O, Aizawa S, Nagai R, Tobe K, Kitamura S, Kadowaki T** 1999 PPARγ mediates high-fat diet-induced adipocyte hypertrophy and insulin resistance. Mol Cell 4:597–609
6. **Bronner F** 2001 Extracellular and intracellular regulation of calcium homeostasis. Scientific World Journal 1:919–925
7. **Vazquez M, Silvestre JS, Prous JR** 2002 Experimental approaches to study PPARγ agonists as antidiabetic drugs. Methods Find Exp Clin Pharmacol 24:515–523
8. **Tanaka H, Teitelbaum SL** 1990 Vitamin D regulates transferrin receptor expression by bone marrow macrophage precursors. J Cell Physiol 145:303–309
9. **Selvaraj P, Chandra G, Jawahar MS, Rani MV, Rajeshwari DN, Narayanan PR** 2004 Regulatory role of vitamin D receptor gene variants of *BsmI*, *ApaI*, *TaqI*, and *FokI* polymorphisms on macrophage phagocytosis and lymphoproliferative response to mycobacterium tuberculosis antigen in pulmonary tuberculosis. J Clin Immunol 24:523–532
10. **Moore KJ, Rosen ED, Fitzgerald ML, Randow F, Andersson LP, Altshuler D, Milstone DS, Mortensen RM, Spiegelman BM, Freeman MW** 2001 The role of PPARγ in macrophage differentiation and cholesterol uptake. Nat Med 7:41–47
11. **Fitzgerald ML, Moore KJ, Freeman MW** 2002 Nuclear hormone receptors and cholesterol trafficking: the orphans find a new home. J Mol Med 80:271–281
12. **Holmgren A** 1985 Thioredoxin. Annu Rev Biochem 54:237–271
13. **Masutani H, Yodoi J** 2002 Thioredoxin. Overview. Methods Enzymol 347: 279–286
14. **Nishiyama A, Matsui M, Iwata S, Hirota K, Masutani H, Nakamura H, Takagi Y, Sono H, Gon Y, Yodoi J** 1999 Identification of thioredoxin-binding protein-2/vitamin D(3) up-regulated protein 1 as a negative regulator of thioredoxin function and expression. J Biol Chem 274:21645–21650
15. **Chen KS, DeLuca HF** 1994 Isolation and characterization of a novel cDNA from HL-60 cells treated with 1,25-dihydroxyvitamin D-3. Biochim Biophys Acta 1219:26–32
16. **Ikarashi M, Takahashi Y, Ishii Y, Nagata T, Asai S, Ishikawa K** 2002 Vitamin D3 up-regulated protein 1 (VDUP1) expression in gastrointestinal cancer and its relation to stage of disease. Anticancer Res 22:4045–4048
17. **Butler LM, Zhou X, Xu WS, Scher HI, Rifkind RA, Marks PA, Richon VM** 2002 The histone deacetylase inhibitor SAHA arrests cancer cell growth, up-regulates thioredoxin-binding protein-2, and down-regulates thioredoxin. Proc Natl Acad Sci USA 99:11700–11705
18. **Han SH, Jeon JH, Ju HR, Jung U, Kim KY, Yoo HS, Lee YH, Song KS, Hwang HM, Na YS, Yang Y, Lee KN, Choi I** 2003 VDUP1 upregulated by TGF-β1 and 1,25-dihydorxyvitamin D3 inhibits tumor cell growth by blocking cell-cycle progression. Oncogene 22:4035–4046
19. **Nishinaka Y, Nishiyama A, Masutani H, Oka S, Ahsan KM, Nakayama Y, Ishii Y, Nakamura H, Maeda M, Yodoi J** 2004 Loss of thioredoxin-binding protein-2/vitamin D3 up-regulated protein 1 in human T-cell leukemia virus type I-dependent T-cell transformation: implications for adult T-cell leukemia leukemogenesis. Cancer Res 64:1287–1292
20. **Nishinaka Y, Masutani H, Oka S, Matsuo Y, Yamaguchi Y, Nishio K, Ishii Y, Yodoi J** 2004 Importin α1 (Rch1) mediates nuclear translocation of thioredoxin-binding protein-2/vitamin D(3)-up-regulated protein 1. J Biol Chem 279:37559–37565

21. **Bodnar JS, Chatterjee A, Castellani LW, Ross DA, Ohmen J, Cavalcoli J, Wu C, Dains KM, Catanese J, Chu M, Sheth SS, Charugundla K, Demant P, West DB, de Jong P, Lusis AJ** 2002 Positional cloning of the combined hyperlipidemia gene Hyplip1. Nat Genet 30:110–116
22. **Hui TY, Sheth SS, Diffley JM, Potter DW, Lusis AJ, Attie AD, Davis RA** 2004 Mice lacking thioredoxin-interacting protein provide evidence linking cellular redox state to appropriate response to nutritional signals. J Biol Chem 279: 24387–24393
23. **Oka S, Liu W, Masutani H, Hirata H, Shinkai Y, Yamada SI, Yoshida T, Nakamura H, Yodoi J,** Impaired fatty acid utilization in Thioredoxin binding protein-2 (TBP-2)-deficient mice: a unique animal model of Reye syndrome. FASEB J, published online Oct 27, 2005
24. **Ohshima T, Koga H, Shimotohno K** 2004 Transcriptional activity of peroxisome proliferator-activated receptor γ is modulated by SUMO-1 modification. J Biol Chem 279:29551–29557
25. **Kim YC, Yamaguchi Y, Kondo N, Masutani H, Yodoi J** 2003 Thioredoxin-dependent redox regulation of the antioxidant responsive element (ARE) in electrophile response. Oncogene 22:1860–1865
26. **Yamamoto Y, Sakamoto M, Fujii G, Kanetaka K, Asaka M, Hirohashi S** 2001 Cloning and characterization of a novel gene, DRH1, down-regulated in advanced human hepatocellular carcinoma. Clin Cancer Res 7:297–303
27. **Strausberg RL, Feingold EA, Grouse LH, Derge JG, Klausner RD, Collins FS, Wagner L, Shenmen CM, Schuler GD, Altschul SF, Zeeberg B, Buetow KH, Schaefer CF, Bhat NK, Hopkins RF, Jordan H, Moore T, Max SI, Wang J, Hsieh F, Diatchenko L, Marusina K, Farmer AA, Rubin GM, Hong L, *et al.*** 2002 Generation and initial analysis of more than 15,000 full-length human and mouse cDNA sequences. Proc Natl Acad Sci USA 99:16899–16903
28. **Rosen ED, Sarraf P, Troy AE, Bradwin G, Moore K, Milstone DS, Spiegelman BM, Mortensen RM** 1999 PPARγ is required for the differentiation of adipose tissue *in vivo* and *in vitro*. Mol Cell 4:611–617
29. **Tontonoz P, Nagy L, Alvarez JG, Thomazy VA, Evans RM** 1998 PPARγ promotes monocyte/macrophage differentiation and uptake of oxidized LDL. Cell 93:241–252
30. **Pizzimenti S, Laurora S, Briatore F, Ferretti C, Dianzani MU, Barrera G** 2002 Synergistic effect of 4-hydroxynonenal and PPAR ligands in controlling human leukemic cell growth and differentiation. Free Radic Biol Med 32:233–245
31. **Kota BP, Huang TH, Roufogalis BD** 2005 An overview on biological mechanisms of PPARs. Pharmacol Res 51:85–94
32. **Joguchi A, Otsuka I, Minagawa S, Suzuki T, Fujii M, Ayusawa D** 2002 Overexpression of VDUP1 mRNA sensitizes HeLa cells to paraquat. Biochem Biophys Res Commun 293:293–297
33. **Lee CH, Olson P, Evans RM** 2003 Minireview: lipid metabolism, metabolic diseases, and peroxisome proliferator-activated receptors. Endocrinology 144: 2201–2207
34. **Merkel M, Eckel RH, Goldberg IJ** 2002 Lipoprotein lipase: genetics, lipid uptake, and regulation. J Lipid Res 43:1997–2006
35. **Claing A, Laporte SA, Caron MG, Lefkowitz RJ** 2002 Endocytosis of G protein-coupled receptors: roles of G protein-coupled receptor kinases and β-arrestin proteins. Prog Neurobiol 66:61–79
36. **Chen W, Kirkbride KC, How T, Nelson CD, Mo J, Frederick JP, Wang XF, Lefkowitz RJ, Blobe GC** 2003 β-Arrestin 2 mediates endocytosis of type III TGF-β receptor and down-regulation of its signaling. Science 301:1394–1397
37. **Luttrell LM, Lefkowitz RJ** 2002 The role of β-arrestins in the termination and transduction of G-protein-coupled receptor signals. J Cell Sci 115:455–465
38. **Haussler CA, Marion SL, Pike JW, Haussler MR** 1986 1,25-Dihydroxyvitamin D3 inhibits the clonogenic growth of transformed cells via its receptor. Biochem Biophys Res Commun 139:136–143
39. **Sasaki T, Fujimoto Y, Tsuchida A, Kawasaki Y, Kuwada Y, Chayama K** 2001 Activation of peroxisome proliferator-activated receptor γ inhibits the growth of human pancreatic cancer. Pathobiology 69:258–265
40. **Nishinaka Y, Masutani H, Nakamura H, Yodoi J** 2001 Regulatory roles of thioredoxin in oxidative stress-induced cellular responses. Redox Rep 6:289–295
41. **Teis D, Huber LA** 2003 The odd couple: signal transduction and endocytosis. Cell Mol Life Sci 60:2020–2033
42. **Pignatelli M, Cortes-Canteli M, Lai C, Santos A, Perez-Castillo A** 2001 The peroxisome proliferator-activated receptor γ is an inhibitor of ErbBs activity in human breast cancer cells. J Cell Sci 114:4117–4126
43. **Gelman L, Michalik L, Desvergne B, Wahli W** 2005 Kinase signaling cascades that modulate peroxisome proliferator-activated receptors. Curr Opin Cell Biol 17:216–222

Endocrinology **is published monthly by The Endocrine Society (http://www.endo-society.org), the foremost professional society serving the endocrine community.**

RONBON 2

論 文

低酸素を標的とした生体イメージング分子プローブの開発

京都大学大学院医学研究科、放射線腫瘍学・画像応用治療学 COE助教授 近藤科江
京都大学大学院医学研究科、放射線腫瘍学・画像応用治療学 教授 平岡眞寛

はじめに

三大死因である「がん」「心疾患」「脳血管疾患」の全死因における割合は、1935年には17.6%だったものが1970年には54.7%、1990年には61.6%に急増している[1]。これらの疾患に共通するキーワードが『低酸素』である。生体内に潜む異常な低酸素状態を確実に、感度良くイメージするプローブを開発することができれば、上記三大疾患の早期発見を可能にし、早期治療や、新規治療法の開発に貢献できる。心筋梗塞・脳梗塞などの虚血性疾患における『低酸素』は、広く知られている。梗塞部位周辺の組織細胞が低酸素状態にあるうちに発見し、治療することができれば、死亡率を減らすことができると共に、予後を大幅に改善できる。がんにおける『低酸素』は、あまり知られていないが、固形がんには低酸素領域が存在し（**図1**）、悪性度の高いがんでより多く含まれていることが臨床で報告されている。また、1mm以下の微小ながんにも、低酸素領域が存在することが、動物実験で示されており、初期のがんや転移がんの早期発見のための良い標的になる。特定の臓器がんに特徴的な分子を標的にする『分子標的』は、特定のがんを治療する上では、非常に有効で、臨床上も大きな成果をあげつつある。一方で、どこにできるかわからない「がん」を早期に発見・治療するためには、がんに共通して存在し、かつ正常組織には存在しない特徴を標的にする必要がある。固形がんに共通して存在する『低酸素』は、正常組織には存在しないため、最適な標的と考えられる。もう一歩進めて、人間ドックのような集団検診で『低酸素』を調べることができるようなイメージングプローブを開発できれば、上記三大疾病を同時に検査することが可能になるかもしれない。我々は、そのようなイメージングプローブの開発をめざし、低酸

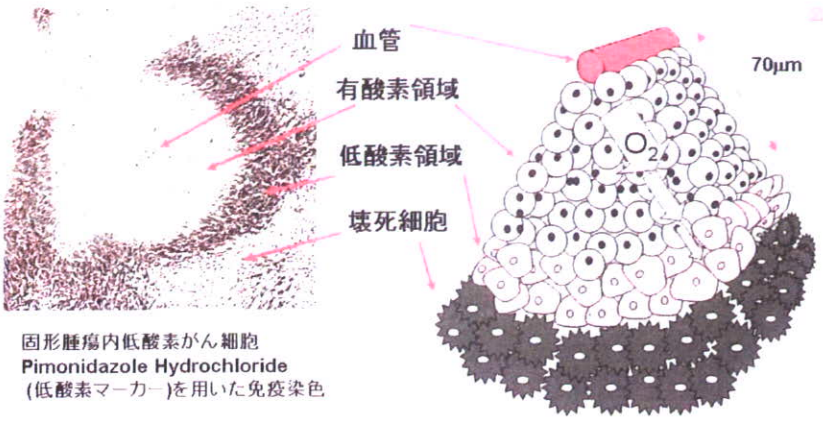

左は、腫瘍切片を低酸素マーカーpimonidazoleを用いて免疫染色し、腫瘍内低酸素領域(茶色)を染めた。右は、腫瘍の構造を模式的に示した。血管からの距離が大きくなるにつれて、酸素や栄養濃度が低くなり、pimonidazoleで認識されるような低酸素状態となり、それを越えると酸素も栄養も枯渇して細胞は死んでしまう。

HIF-1タンパク質は、HIF-1αとHIF-1βの二量体からなる転写因子で、低酸素応答遺伝子の転写制御領域にあるHRE(hypoxia responsive element)に結合して、図(下)に示している様な様々な機能をもつ遺伝子の転写を誘導する。HIF-1αは、低酸素状態の細胞内では安定して存在する(左上)が、有酸素状態の細胞では図内の1~4の反応によって速やかに分解される(右上)。1. プロリン水酸化酵素によりODDドメイン内のプロリン残基が水酸化される。2. その修飾をユビキチン連結酵素複合体E3が認識して、VHLを介して結合し、3. HIF-1αはユビキチン化される。4. ユビキチン化されたHIF-1αは、プロテアソームに運ばれ分解される。

素に特異的に安定化する融合蛋白質を応用したイメージングプローブを構築している。

酸素濃度依存的なタンパク質安定性制御機構

低酸素状態にある細胞には、極めて興味深いタンパク質が存在する。そのタンパク質はHIF-1αと呼ばれ、転写因子HIF-1を構成する2つのサブユニットのひとつで、低酸素環境で安定化し、通常の酸素環境下(有酸素環境)で速やかに分解される[2]。すなわち、HIF-1は低酸素環境下で特異的に安定化して、転写因子として機能し、一連の低酸素応答遺伝子の発現を誘導する(図2)。それらの遺伝子は、低酸素細胞が過酷な環境に順応するために必要な因子やがんの悪性化に関与する因子をコードしており、現在までに40以上の遺伝子が報告されている[3]。

我々は、HIF-1αタンパク質の酸素濃度依存的分解(ODD:oxygen-dependent degradation)機構に着目した。この制御機構は、2001年にプロリン水酸化酵素がクローニングされることによって、ほぼ全貌が解明された[4]。即ち、有酸素状態では、プロリン水酸化酵素が、HIF-1α